DISSIPATIVITY AND PERFORMANCE ANALYSIS OF SMART DAMPERS VIA LMI SYNTHESIS

Erik A. Johnson[1], Associate Member, ASCE and Baris Erkus[2], Student Member, ASCE

ABSTRACT

This paper investigates the dissipativity and performance of semiactive systems with smart dampers via linear matrix inequality (LMI) synthesis. For this purpose, a dissipativity index is proposed to modify a standard linear quadratic regulator (LQR) using the techniques available in LMI-based multiobjective convex programming for better semiactive performance. First, a review of available dissipativity indices is given, and two new dissipativity indices based on the concept of energy dissipation rate are defined. Second, an LQR problem is defined in terms of a linear objective function and several LMI constraints. Then, for each dissipativity index, a dissipativity inequality constraint is defined. It is observed that only one of the dissipativity constraints can be represented in terms of LMIs and implemented in the LQR problem. A modified LMI-based LQR controller is obtained by attaching the dissipativity constraint in its weak form. The dissipativity indices and the proposed controller are employed for two numerical examples to investigate the dissipativity and performance of semiactive systems. The first example is a 2DOF building with an ideal damper attached in the first story, and an LQR controller is selected such that it has high dissipativity levels. The second example is a 2DOF model of a highway bridge where a realistic magnetorheological (MR) fluid damper is attached at the bearing location resulting in an LQR controller with low dissipativity levels. Comprehensive parametric studies are carried out for both examples using the modified LQR with various dissipativity constraint values and the standard LQR. For the first example, it is found that the indices are very useful to identify the dissipative nature and semiactive performance relations. Also, the proposed method is able to improve the dissipative nature of the controller improving the semiactive performance. On the other hand, for the second example, although the proposed method is able to improve the dissipativity, the overall semiactive performance does not show a major improvement due to drastically lowered dissipativity levels caused by the realistic damper model.

Keywords: dissipativity, smart dampers, semiactive control, linear quadratic regulator, linear matrix inequalities.

---

1. Asst. Prof., Dept. of Civil and Env. Engrg., Univ. of Southern California, Los Angeles, CA 90089-2531; JohnsonE@usc.edu
2. Ph. D. Student, Dept. of Civil and Env. Engrg., Univ. of Southern California, Los Angeles, CA 90089-2531; erkus@usc.edu

INTRODUCTION

Smart dampers constitute an important class of semiactive devices used for structural control and vibration mitigation in civil engineering (Housner *et al*. 1997; Spencer and Sain 1997; Symans and Constantinou 1999; Soong and Spencer 2002). These devices are controllable dampers and, thus, have the fundamental physical property of a simple mechanical damper (e.g., a simple dashpot element): they dissipate energy from the system to which they are attached. While this property makes smart dampers very attractive from the point of view of robustness, it limits their performance compared to active devices that can also inject energy into the controlled system. This limitation stands as an important problem in the design of semiactive control systems since there are no well-established analytical control strategies that accommodate the type of nonlinearity caused by the dissipative nature of a smart damper.

An often-employed semiactive control strategy for smart-dampers is clipped optimal control (Dyke *et al.* 1996; Spencer *et al*. 2000; Erkus *et al.* 2002; Ramallo et al. 2002; Johnson *et al*. 2004). Clipped optimal control assumes that the structure is linear and the control device is fully active. It then employs linear active control theory to design a primary controller, and a clipping algorithm is used as a secondary controller to make the damper mimic an active device and produce a force close to that commanded by the primary controller (Fig. 1). The primary controller is generally a linear quadratic (LQ) optimal controller since this class of control theory is well-known and widely applied in structural control. In the past decade, it has been shown by several researchers that a clipped optimal control strategy with a smart damper, such as a magnetorheological (MR) fluid damper, is quite effective and demonstrates results competitive to a corresponding active control strategy.

The effectiveness of a smart damper commanded by the clipped optimal control strategy can be explained by the primary control force being highly dissipative and, thus, suitable for the damper to mimic. In a narrow sense, the dissipative nature of a smart damper can be characterized by a simple nonlinear inequality given by $u_d v_d < 0$, where u_d is the damper force and v_d is the velocity across the damper (see the Appendix for a note on the other definitions on dissipativity). Similarly, a dissipative primary control force can be defined as $u_a v_d < 0$,

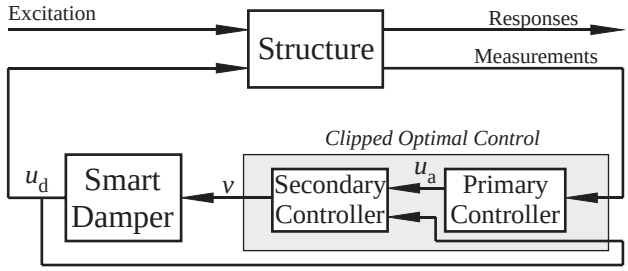

u_a: active control force, v: command parameter (e.g. voltage), u_d: damper force

FIG. 1 A simplified representation of clipped optimal control strategy

where u_a is the primary control force. This inequality simply states that the energy dissipation rate of the primary control force is negative. Therefore, if a fully active device is commanded by a control force $u_a v_a < 0$ during a time period Δt (v_a being the velocity of the point where the device is exerting force), the device will dissipate energy from the structure during Δt. In general, one cannot enforce the condition $u_a v_d < 0$ on the primary controller of an LQ based clipped optimal control strategy, and the dissipative nature of the controller is arbitrary. For example, the dissipativity condition is mostly satisfied for multi-story buildings where the controller is placed in the first floor or in between the base and the ground (Dyke *et al*. 1996, 1998). There are other systems and control designs where the controller must add energy to the structural system to achieve a specific set of design objectives, and the primary controller may command mostly nondissipative forces; e.g., highway bridges and low-mass secondary systems (Inoudi 2000, Erkus *et al.* 2002). Both types of examples show that the dissipative nature of the primary controller is an important characteristics that should be investigated to understand and predict the performance of a semiactive system with a smart damper commanded by a clipped optimal control algorithm. Insight into the concept of dissipativity may also help to develop methods to modify the primary controller so that designers can alter the dissipativity of the controller to get uppermost performance from a smart damper.

In the literature, there is very little work that investigates the dissipative characteristics of the primary controller in a clipped optimal control strategy. This is particularly due to the absence of well defined indices that can measure the dissipativity of the primary control force. Inaudi (2000) proposed a stochastic index that estimates the probability of the primary control force being dissipative, *i.e.,* $P[u_a v < 0]$. Later, Christenson (2003) justified the correlation between $P[u_a v < 0]$ and the performance of the semiactive systems by implementing several numerical examples. Simple deterministic indices based on the dynamic time-history analyses are also used to observe the effect of the dissipative nature of the control force and the ability of damper to mimic the control force (*e.g.*, Erkus *et al.* 2002).

From a practical point of view, a stochastic index gives a broader sense of the dissipativity of a controller in the design stage without time-consuming simulations, whereas a deterministic index is useful to investigate a specific controller for a specific excitation. A stochastic index, however, has a more crucial advantage over a deterministic index: it can be used in conjunction with special methods, such as convex multiobjective techniques, to obtain controllers with various dissipativity levels. These methods are quite popular in the control field, since they allow numerical solution of multiobjective optimal control problems that do not have analytical solution. In fact, numerical solution of these problems are straightforward if

they can be represented as eigenvalue problems in terms of special matrix functions known as linear matrix inequalities (LMIs). On the other hand, for problems that cannot be represented in terms of LMIs, a solution is not always guaranteed, and more sophisticated methods should be employed. Whether they yield numerically solvable problems or not, convex multiobjective techniques are quite helpful for giving insight into very complex problems that cannot be investigated analytically, and can also be used to investigate dissipativity employing stochastic dissipativity indices.

This paper investigates the dissipativity and performance of semiactive systems by proposing two dissipativity indices for the primary controller of a clipped optimal control strategy and utilizing a modified LQR controller to achieve controllers with various dissipativity characteristics. First, available dissipativity indices are reviewed, and proposed dissipativity indices are defined. Then, an LQ problem is represented as an optimization problem with convex LMIs, which is in the form of an eigenvalue problem (EVP). It is observed that one of the proposed dissipativity indices can be represented in weak form as an LMI constraint and can be appended to the LQ problem. The modified LQR controller is implemented on two structures to observe the index–performance relations for several dissipativity levels and controller parameters: (1) a two-degree-of-freedom shear structure (2DOF) with an ideal semiactive damper attached between the first and second stories, and (2) a simplified 2DOF highway bridge model similar to the one given by Erkus *et al.* (2002) with an MR fluid damper (Yang *et al.*, 2002) in the isolation layer below the deck. The results are presented in tabular and graphical forms. Herein, the controller is a state-feedback LQR controller, yet an estimator, such as a Kalman filter, can easily be utilized to estimate the states using the measurements. The MATLAB® LMI Control Toolbox (Gahinet *et al.* 1995) is used as the LMI solver.

DISSIPATIVITY INDICES

In this section, a review of the available dissipativity indices are given, and proposed dissipativity indices are defined. For this purpose, first, a formal definition of a dissipative force is given.

Strictly Dissipative Force

Consider a continuous external force $f(x, t)$, which is applied to a system on a surface region $x \in \Omega$. Let $v(x, t)$ be the velocity of the surface (with positive velocity in the same direction as positive forces). The *rate of energy added* to the system by the force $f(x, t)$ is given by

$$\frac{\partial E}{\partial t} = \int_{\Omega} f(x, t)v(x, t)d\Omega . \tag{1}$$

$f(x, t)$ is called a *strictly dissipative force* if the rate of energy added is negative for all $t \geq 0$. Or, without loss of generality,

$$\int_{\Omega} f(x, t)v(x, t)d\Omega \leq \varepsilon(t) < 0, \quad \text{for all} \quad t \geq 0 \Leftrightarrow f(x, t) \text{ is strictly dissipative} \tag{2}$$

where $\varepsilon(t)$ is a strictly negative real function.

When the external force is a point load applied at point x_0 on the system, (2) simplifies to

$$f(t)v(t) \leq \varepsilon(t) < 0, \quad \text{for all} \quad t \geq 0 \Leftrightarrow f(t) \text{ is strictly dissipative} , \tag{3}$$

where $v(t)$ is the velocity of point x_0, and the location parameter x_0 is dropped for simplicity. Definition given by (3) is more suitable for a control problem since the control force is generally modelled as a point load. This condition simply states that the directions of the force and the velocity are always opposite. In fact, this is the case for a damper. Therefore, a damper force is a strictly dissipative force, and the rate it injects into the system is always negative (*i.e.*, it is always dissipating energy). In this paper, the term *dissipative force* is used instead of *strictly dissipative force* for convenience.

Percentage of Dissipative Control Forces

The following deterministic index computes the percentage of the time that the primary control force commands dissipative forces:

$$D_{\%} = \left(1 - \frac{1}{T}\int_{0}^{T} H[u_{\mathrm{a}}v_{\mathrm{d}}]dt\right) \times 100 \tag{4}$$

where $H(\cdot)$ is the Heaviside unit step function. Since this index is deterministic, a discrete time representation is useful. For a time step $\Delta t = T/N$, $D_{\%}$ can be written as

$$D_{\%} = \left(1 - \frac{1}{N}\sum_{k=0}^{N-1} H[u_{\mathrm{a}}(k\Delta t)v_{\mathrm{d}}(k\Delta t)]\right) \times 100 \tag{5}$$

where $u_{\mathrm{a}}(k\Delta t)$ and $v_{\mathrm{d}}(k\Delta t)$ are the control force and the damper force at the time $k\Delta t$. The higher D-value shows that the control force produces more dissipative forces.

Probability that the Control Force is Dissipative

For a linear system with stationary Gaussian responses, the probability that the control force is strictly dissipative is given by (Inaudi 2000)

$$D_{\mathrm{p}} = P[u_{\mathrm{a}} v_{\mathrm{d}}] = \frac{\operatorname{acos}(\rho_{u_{\mathrm{a}} v_{\mathrm{d}}})}{\pi} \tag{6}$$

where $\rho_{u_{\mathrm{a}} v_{\mathrm{d}}}$ is the correlation coefficient between u_{a} and v_{d}. For a linear system and a linear controller, $\rho_{u_{\mathrm{a}} v_{\mathrm{d}}}$ is the off-diagonal term of the symmetric covariance matrix of the output $\mathbf{z} = [u_{\mathrm{a}} \quad v_{\mathrm{d}}]^{\mathrm{T}}$.

Expected Value of the Energy Flow Rate

As discussed previously, since the dissipative force condition given by (3) is not stochastic, it cannot be directly used to examine a stochastic controller. Therefore, the expected value of this condition is applied to the primary control force as follows:

$$E[u_{\mathrm{a}}(t) v_{\mathrm{d}}(t)] \le E[\varepsilon(t)] = \mu_{\varepsilon}(t) < 0 \Leftarrow u_{\mathrm{a}}(t) \text{ is strictly dissipative}. \tag{7}$$

Note that $E[u_{\mathrm{a}} v_{\mathrm{d}}] < 0$ does not necessarily mean that the control force is strictly dissipative or mostly strictly dissipative. However, it is clear that for values of $E[u_{\mathrm{a}} v_{\mathrm{d}}] \ll \mu_{\varepsilon}(t)$, u_{a} has a higher mean energy flow rate, which can be used as an indication of the dissipative nature of the control force. Therefore the following index is proposed:

$$D_{\mathrm{e}} = E[u_{\mathrm{a}} v_{\mathrm{d}}]. \tag{8}$$

D_{e} is called the *mean energy flow rate* in this paper.

One problem with D_{e} is that it is not unitless; *i.e.*, a large magnitude of D_{e} may be an indication of very large values of force u_{a}. To avoid this problem, a normalized index is also proposed as follows:

$$D_{\mathrm{ne}} = \frac{E[u_{\mathrm{a}} v_{\mathrm{d}}]}{\sqrt{E[u_{\mathrm{a}}^2]}\sqrt{E[v_{\mathrm{d}}^2]}}. \tag{9}$$

D_{ne} is called the *normalized mean energy flow rate* in this paper. Clearly, a negative value of D_{ne} indicates the likelihood of the control force being strictly dissipative.

The Relation Between D_p and D_{ne} for an LQ Problem

In a standard LQ problem, all stochastic variables are zero-mean. Therefore, D_{ne} is, in fact, the correlation coefficient between the force u_a and the velocity v_d, *i.e.*, $D_{ne} = \rho_{u_a v_d}$. Therefore, $-1 \le D_{ne} \le 1$ holds. Moreover, if $-1 \le D_{ne} < 0$ holds, the controller is more likely to produce strictly negative control forces since the denominator of D_{ne} is always positive. Also note that for $-1 \le D_{ne} < 0$, the probability index becomes $0.5 < D_p \le 1$ as shown in Fig. 2. On the other hand, if $0 < D_{ne} \le 1$, the controller force is more likely to add energy to the system and $0 \le D_p < 0.5$.

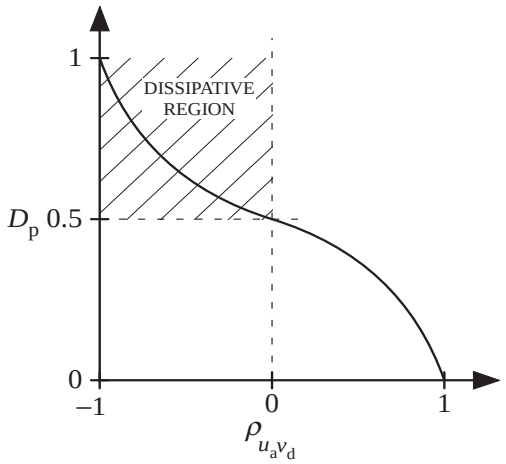

FIG. 2 Relation between D_p and $\rho_{u_a v_d}$.

LMI-EVP REPRESENTATION OF AN LQR PROBLEM

In this section, first, a brief mathematical background is given for LMI analysis. Second, a method for the LMI characterization of a multiobjective optimization problem is summarized. Then, a definition of a standard linear quadratic regulator (LQR) problem is given, and it's LMI characterization is obtained using the method summarized.

Mathematical Background

Linear Matrix Inequalities

The matrix inequality

$$\mathbf{F}(\mathbf{x}) = \mathbf{F}_0 + x_1\mathbf{F}_1 + \ldots + x_n\mathbf{F}_n > 0 \tag{10}$$

is called a *linear matrix inequality*, where $\mathbf{F}(\mathbf{x})$ is an affine function (see the Appendix) of the real vector $\mathbf{x} = [x_1 \;\; x_2 \;\ldots\; x_n]^T$ and $\mathbf{F}_0$, $\mathbf{F}_1$, …, $\mathbf{F}_n$ are real symmetric matrices.

- The inequality $\mathbf{F}(\mathbf{x}) > 0$ implies that $\mathbf{F}(\mathbf{x})$ is a positive definite matrix, *i.e.*, the real parts of all eigenvalues of $\mathbf{F}(\mathbf{x})$ are positive.
- A vector $\mathbf{x}$ that satisfies the inequality (10) is known as a feasible solution of the LMI. The feasible solution set of the inequality (10), $\{\mathbf{x} \,|\, \mathbf{F}(\mathbf{x}) > 0\}$, is a convex set (see the Appendix). Convexity is an

important property since there are powerful numerical techniques for the solution of problems with convex solution sets (Boyd *et al*. 1994; Nesterov and Nemirovskii 1994).

- Some inequalities not in the form of (10) can be converted to LMIs by some algebraic operations. Also, multiple LMIs can be represented with a single equivalent LMI by defining a new variable that includes the variables of the multiple LMIs. Further, the solution set of some nonconvex matrix inequalities can be mapped into a convex solution set of a corresponding LMI. Therefore, a problem that cannot be solved analytically or numerically, due to several types of inequalities, can be solved numerically if these inequalities can be converted into LMIs.
- Often encountered in control problems are inequalities with matrix variables instead of a vector as given in inequality (10). As an example, consider the Lyapunov inequality $\mathbf{AP} + \mathbf{PA}^{\mathrm{T}} < 0$ where $\mathbf{A}$ is a given (known) matrix and the symmetric real matrix $\mathbf{P}$ is the variable. This inequality can easily be reduced into the form given by inequality (10) (Boyd *et al*. 1994). In this paper, these type of LMIs will not be explicitly reduced to vector form of (10); rather, they will be used as they are.

Bilinear Matrix Inequalities

The inequality

$$\mathbf{F}(\mathbf{x}, \mathbf{y}) > 0 \tag{11}$$

is called a *bilinear matrix inequality* and the matrix valued function $\mathbf{F}(\mathbf{x}, \mathbf{y})$ is called bilinear if $\mathbf{F}(\mathbf{x}, \mathbf{y})$ is affine with respect to each of its arguments; *i.e.*, $\mathbf{F}(\mathbf{x}, \mathbf{y})$ is affine in $\mathbf{x}$ when $\mathbf{y}$ is fixed and vice versa.

- BMIs are, in general, nonconvex and have an intractable computational complexity known as $\mathcal{NP}$-hardness (Toker and Özbay 1995). Therefore, there are no efficient algorithms for the numerical solution of problems involving BMIs. However, by defining new variables, some BMIs can be converted to equivalent LMIs; i.e, a new LMI is defined whose solution set can be mapped into the solution set of the BMI. This property is important since BMIs are frequently encountered in control problems.

Stability and Lyapunov's Equality

There are various interpretations of stability in the general field of civil engineering. In this paper, stability refers to bounded-input-bounded-output (BIBO) stability (see, e.g., Chen 1999 for a definition and treatment of BIBO stability). A linear time-invariant system given by $\dot{\mathbf{q}} = \mathbf{Aq}$ is stable if every eigenvalue of $\mathbf{A}$ has a negative real part (Chen 1999); a matrix $\mathbf{A}$ satisfying this condition is called *Hurwitz*. A convenient way to check the eigenvalues of $\mathbf{A}$ is to employ a Lyapunov equation as follows: All eigenval-

ues of $\mathbf{A}$ have negative real parts if and only if, for any given matrix $\mathbf{Q} = \mathbf{Q}^{\mathrm{T}} > 0$, there exists a unique solution $\mathbf{S} = \mathbf{S}^{\mathrm{T}} > 0$ for the Lyapunov equation given by $\mathbf{AS} + \mathbf{SA}^{\mathrm{T}} = -\mathbf{Q}$ (or $\mathbf{A}^{\mathrm{T}}\mathbf{S} + \mathbf{SA} = -\mathbf{Q}$). This condition can also be stated as follows: The system $\dot{\mathbf{q}} = \mathbf{Aq}$ is stable (and $\mathbf{A}$ is Hurwitz) if the LMI $\mathbf{AS} + \mathbf{SA}^{\mathrm{T}} + \mathbf{Q} \le 0$, or its strict version $\mathbf{AS} + \mathbf{SA}^{\mathrm{T}} + \mathbf{Q} < 0$, has a feasible solution $\mathbf{S} = \mathbf{S}^{\mathrm{T}} > 0$ (see, e.g., Slotine and Li (1991) for a treatment of Lyapunov stability theory). Herein, $\mathbf{S}$ is called the Lyapunov matrix.

There are other useful properties of the Lyapunov equality. For example, the solution of the Lyapunov equation will simply give the controllability and observability grammians for a specific value of $\mathbf{Q} = \mathbf{Q}^{\mathrm{T}} > 0$ (see, e.g., Dullerud and Paganini (2000) for the definitions and derivations). Similarly, for a given system $\dot{\mathbf{q}} = \mathbf{Aq} + \mathbf{Ew}$, where $\mathbf{w}$ is a white noise external disturbance with unit intensity $E[\mathbf{w}(t)\mathbf{w}^{\mathrm{T}}(t+\tau)] = \mathbf{I}\delta(\tau)$, the solution of the Lyapunov equation for $\mathbf{Q} = \mathbf{EE}^{\mathrm{T}}$ is simply the expected value of $\mathbf{qq}^{\mathrm{T}}$ (*i.e.*, the covariance matrix of the states $\mathbf{q}$).

LMI Characterization of Multivariable Feedback Control Systems

In a very broad sense, multivariable feedback control deals with problems with more than one design objective including time and frequency domain constraints (see, e.g., Scherer *et al*. (1997) for a list of designs objectives encountered frequently in the field of control). In most cases, an analytical solution for a controller that satisfies multiple constraints is not available. To obtain an LMI characterization for these types of problems, a method is given by Scherer *et al*. (1997) and is very briefly summarized here:

- Consider a closed-loop system $\dot{\mathbf{q}}_{\mathrm{c}} = \mathbf{A}_{\mathrm{c}}\mathbf{q}_{\mathrm{c}}$, where $\mathbf{A}_{\mathrm{c}}$ is Hurwitz and is a function of the controller. Let $\mathbf{S}$ be the Lyapunov matrix for this closed loop system satisfying the Lyapunov inequality. For each of the objectives, a matrix inequality condition in terms of a Lyapunov matrix is found. Inequality conditions are selected such that they are satisfied when the corresponding design specification is met. The final inequalities become a function of $\mathbf{A}_{\mathrm{c}}$, the controller and the Lyapunov matrix. Therefore, these matrix inequalities are, in general, bilinear.
- Let the matrix inequality condition associated with the i^{th} objective be $\mathbf{F}_i(\mathbf{K}, \mathbf{S}_i) > 0$, where $\mathbf{S}_i$ is the corresponding Lyapunov matrix and $\mathbf{K}$ is the controller. Then, to enforce a unique Lyapunov matrix for the system, all the Lyapunov matrices are set to a single Lyapunov matrix as $\mathbf{S}_1 = \ldots = \mathbf{S}_N = \mathbf{S}$. Therefore, a problem with several BMIs, whose Lyapunov matrices are all $\mathbf{S}$, is obtained.
- The final step is to introduce new variables or to employ some algebraic manipulations to convert BMIs into LMIs. After obtaining an LMI for each constraint, all LMIs are cast into a single large LMI.

After these manipulations, the final problem will have a convex LMI constraint and can be solved numerically. It should be noted that the mapping between the BMIs and LMIs must be one-to-one.

If the problem includes an optimization criteria, the LMI problem is generally in the form of an eigenvalue problem (Boyd *et al*. 1994). An eigenvalue problem has several representations. The one that will be employed in this paper is as follows:

$$\begin{aligned} &\min_{\mathbf{x}} \ \mathbf{c}^{\mathrm{T}}\mathbf{x} \\ &\text{subject to } \mathbf{F}(\mathbf{x}) > 0 \end{aligned} \tag{12}$$

where $\mathbf{c}$ is a known vector and $\mathbf{F}(\mathbf{x}) > 0$ is an LMI. Clearly, the object function $\mathbf{c}^{\mathrm{T}}\mathbf{x}$ is a linear function of $\mathbf{x}$, and the constraint $\mathbf{F}(\mathbf{x}) > 0$ is a convex inequality. Another form of EVP has a matrix objective function with terms in the form of $\mathbf{C}^{\mathrm{T}}\mathbf{X}$ where $\mathbf{C}$ and $\mathbf{X}$ are matrices of appropriate dimensions, which, in fact, can be represented by (12) with some algebraic manipulations (Boyd *et al*. 1994; Gahinet *et al*. 1995).

LQR Control Problem

State-feedback linear quadratic regulator (LQR) control is a frequently used theory in the field of structural control since the background concepts are easily understood, and a proper design can achieve an efficient performance. In this paper, LQR is the baseline control strategy, and is defined as follows. Consider a linear time-invariant system:

$$\begin{aligned} \dot{\mathbf{q}} &= \mathbf{A}\mathbf{q} + \mathbf{B}\mathbf{u} + \mathbf{E}\mathbf{w} \\ \mathbf{z} &= \mathbf{C}_z\mathbf{q} + \mathbf{D}_z\mathbf{u} + \mathbf{F}_z\mathbf{w} \end{aligned} \tag{13}$$

where $\mathbf{q}$ is the state vector, $\mathbf{u}$ is a vector of control forces, $\mathbf{w}$ is a stationary zero-mean white noise stochastic vector process disturbance with unit intensity, and $\mathbf{z}$ is the vector of outputs to be minimized. In structural control, the excitation is generally earthquake ground acceleration or wind excitation modelled as filtered white noise, and the outputs are structural response quantities such as story drifts or absolute accelerations that lead to a zero $\mathbf{F}_z$. The LQR problem is to find the control gain $\mathbf{K}$ that satisfies the optimization

$$\begin{aligned} &\min_{\mathbf{K}} \ E[\mathbf{z}^{\mathrm{T}}\tilde{\mathbf{Q}}\mathbf{z} + \mathbf{u}^{\mathrm{T}}\tilde{\mathbf{R}}\mathbf{u} + \mathbf{z}^{\mathrm{T}}\tilde{\mathbf{N}}\mathbf{u} + \mathbf{u}^{\mathrm{T}}\tilde{\mathbf{N}}^{\mathrm{T}}\mathbf{z}] \\ &\text{subject to (13) and } \mathbf{u} = -\mathbf{K}\mathbf{q} \end{aligned} \tag{14}$$

where $\tilde{\mathbf{Q}} = \tilde{\mathbf{Q}}^{\mathrm{T}} \geq 0$, $\tilde{\mathbf{R}} = \tilde{\mathbf{R}}^{\mathrm{T}} > 0$ and $\tilde{\mathbf{N}}$ are weighting matrices, and $\mathbf{K}$ is a constant feedback gain matrix. Substituting the output equation in (13) into the optimization problem (14), one obtains another form of the LQR problem

$$\begin{aligned} &\min_{\mathbf{K}} \; E[\mathbf{q}^{\mathrm{T}}\mathbf{Q}\mathbf{q} + \mathbf{u}^{\mathrm{T}}\mathbf{R}\mathbf{u} + \mathbf{q}^{\mathrm{T}}\mathbf{N}\mathbf{u} + \mathbf{u}^{\mathrm{T}}\mathbf{N}^{\mathrm{T}}\mathbf{q}] \\ &\text{subject to } \; \dot{\mathbf{q}} = \mathbf{A}\mathbf{q} + \mathbf{B}\mathbf{u} + \mathbf{E}\mathbf{w}, \quad \mathbf{u} = -\mathbf{K}\mathbf{q} \end{aligned} \tag{15}$$

where

$$\mathbf{Q} = \mathbf{C}_z^{\mathrm{T}}\tilde{\mathbf{Q}}\mathbf{C}_z, \quad \mathbf{N} = \mathbf{C}_z^{\mathrm{T}}\tilde{\mathbf{Q}}\mathbf{D}_z + \mathbf{C}_z^{\mathrm{T}}\tilde{\mathbf{N}}, \quad \mathbf{R} = \tilde{\mathbf{R}} + \mathbf{D}_z^{\mathrm{T}}\tilde{\mathbf{Q}}\mathbf{D}_z + \mathbf{D}_z^{\mathrm{T}}\tilde{\mathbf{N}} + \tilde{\mathbf{N}}^{\mathrm{T}}\mathbf{D}_z . \tag{16}$$

For the problem defined by (15) and (16) to be well-posed, design parameters should satisfy the following inequalities (see the Appendix for a note on this condition):

$$\mathbf{W} = \begin{bmatrix} \mathbf{Q} & \mathbf{N} \\ \mathbf{N}^{\mathrm{T}} & \mathbf{R} \end{bmatrix} \geq 0 \text{ and } \mathbf{R} > 0 . \tag{17}$$

LMI-EVP Representation of an LQR Problem

A derivation of the LMI-EVP representation of an LQR problem is given utilizing the method given by Scherer *et al*. (1997). Note that other methods to obtain the same representation are available in the control theory literature (see the Appendix). First, the LQR problem is redefined in a form suitable for LMI characterization as follows: consider the LQR problem given by (15) and (16). Let $\mathbf{Q}^{1/2}$ and $\mathbf{R}^{1/2}$ be real symmetric matrices that satisfy $\mathbf{Q}^{1/2}\mathbf{Q}^{1/2} = \mathbf{Q}$ and $\mathbf{R}^{1/2}\mathbf{R}^{1/2} = \mathbf{R}$. Using $\mathbf{u} = -\mathbf{K}\mathbf{q}$, optimization (15) can be written as

$$\begin{aligned} &\min_{\mathbf{K}} \; E[\mathbf{q}^{\mathrm{T}}\mathbf{Q}^{1/2}\mathbf{Q}^{1/2}\mathbf{q} + \mathbf{q}^{\mathrm{T}}\mathbf{K}^{\mathrm{T}}\mathbf{R}^{1/2}\mathbf{R}^{1/2}\mathbf{K}\mathbf{q} - \mathbf{q}^{\mathrm{T}}\mathbf{N}\mathbf{K}\mathbf{q} - \mathbf{q}^{\mathrm{T}}\mathbf{K}^{\mathrm{T}}\mathbf{N}^{\mathrm{T}}\mathbf{q}] \\ &\text{subject to } \; \dot{\mathbf{q}} = (\mathbf{A}-\mathbf{B}\mathbf{K})\mathbf{q} + \mathbf{E}\mathbf{w} \end{aligned} . \tag{18}$$

Let $E[\mathbf{q}\mathbf{q}^{\mathrm{T}}] = \mathbf{P}$, which is the state covariance matrix; clearly, $\mathbf{P} = \mathbf{P}^{\mathrm{T}} > 0$. Utilizing the trace operator $Tr(\cdot)$ and a Lyapunov equation, whose solution gives the state covariance matrix, to represent the stability of the system, optimization (18) can be written as

$$\begin{aligned} &\min_{\mathbf{K},\,\mathbf{P}} \; Tr(\mathbf{Q}^{1/2}\mathbf{P}\mathbf{Q}^{1/2}) + Tr(\mathbf{R}^{1/2}\mathbf{K}\mathbf{P}\mathbf{K}^{\mathrm{T}}\mathbf{R}^{1/2}) - Tr(\mathbf{K}\mathbf{P}\mathbf{N}) - Tr(\mathbf{N}^{\mathrm{T}}\mathbf{P}\mathbf{K}^{\mathrm{T}}) \\ &\text{subject to } \; (\mathbf{A}-\mathbf{B}\mathbf{K})\mathbf{P} + \mathbf{P}(\mathbf{A}-\mathbf{B}\mathbf{K})^{\mathrm{T}} + \mathbf{E}\mathbf{E}^{\mathrm{T}} = 0, \qquad \mathbf{P} = \mathbf{P}^{\mathrm{T}} > 0 \end{aligned} . \tag{19}$$

Having redefined the LQR problem in a form suitable for LMI characterization, the LMI-EVP representation can be found using the first step of the aforementioned method (Scherer *et al*. 1997). For this purpose, the following optimization problem for the closed loop system $\dot{\mathbf{q}} = \mathbf{A}\mathbf{q} + \mathbf{B}\mathbf{u} + \mathbf{E}\mathbf{w}$ and $\mathbf{u} = -\mathbf{F}\mathbf{q}$ is defined:

$$\begin{aligned} &\min_{\mathbf{F},\,\mathbf{S}} \; Tr(\mathbf{Q}^{1/2}\mathbf{S}\mathbf{Q}^{1/2}) + Tr(\mathbf{R}^{1/2}\mathbf{F}\mathbf{S}\mathbf{F}^{\mathrm{T}}\mathbf{R}^{1/2}) - Tr(\mathbf{F}\mathbf{S}\mathbf{N}) - Tr(\mathbf{N}^{\mathrm{T}}\mathbf{S}\mathbf{F}^{\mathrm{T}}) \\ &\text{subject to} \;\; (\mathbf{A}-\mathbf{B}\mathbf{F})\mathbf{S} + \mathbf{S}(\mathbf{A}-\mathbf{B}\mathbf{F})^{\mathrm{T}} + \mathbf{E}\mathbf{E}^{\mathrm{T}} < 0, \qquad \mathbf{S} = \mathbf{S}^{\mathrm{T}} > 0 \end{aligned} \tag{20}$$

where $\mathbf{S}$ is the Lyapunov matrix. It is proposed that the solution of (19) is indeed equivalent to the solution of (20); *i.e.*, if $\mathbf{K}_0$ and $\mathbf{P}_0$ are the solutions to (19), and $\mathbf{F}_0$ and $\mathbf{S}_0$ are the solutions to (20), then $\mathbf{K}_0 = \mathbf{F}_0$ and $\mathbf{P}_0 = \mathbf{S}_0$. Proof of this proposition is given in the Appendix. One should also note that although $\mathbf{S}$ does not represent the state covariance matrix, the solution of (20), $\mathbf{S}_0$, is equal to the state covariance matrix.

The optimization problem (20) is not exactly in the form of the EVP (12) since it includes the multiplicative terms $\mathbf{F}\mathbf{S}$ (*i.e.*, the objective function is not linear), and the first inequality constraint is a BMI (i.e, the constraint is not convex). To convert the BMI constraint into an LMI constraint, a new variable $\mathbf{Y} = \mathbf{F}\mathbf{S}$ is introduced, and (20) becomes

$$\begin{aligned} &\min_{\mathbf{Y},\,\mathbf{S}} \; Tr(\mathbf{Q}^{1/2}\mathbf{S}\mathbf{Q}^{1/2}) + Tr(\mathbf{R}^{1/2}\mathbf{Y}\mathbf{S}^{-1}\mathbf{Y}^{\mathrm{T}}\mathbf{R}^{1/2}) - Tr(\mathbf{Y}\mathbf{N}) - Tr(\mathbf{N}^{\mathrm{T}}\mathbf{Y}^{\mathrm{T}}) \\ &\text{subject to} \;\; \mathbf{A}\mathbf{S}-\mathbf{B}\mathbf{Y} + \mathbf{S}\mathbf{A}^{\mathrm{T}}-\mathbf{Y}^{\mathrm{T}}\mathbf{B}^{\mathrm{T}} + \mathbf{E}\mathbf{E}^{\mathrm{T}} < 0, \qquad \mathbf{S} = \mathbf{S}^{\mathrm{T}} > 0 \end{aligned} . \tag{21}$$

The nonlinear term in the objective function can be represented as the solution to an optimization

$$Tr(\mathbf{R}^{1/2}\mathbf{Y}\mathbf{S}^{-1}\mathbf{Y}^{\mathrm{T}}\mathbf{R}^{1/2}) = \begin{bmatrix} \min\limits_{\mathbf{X}} \; Tr(\mathbf{X}) \\ \text{subject to} \;\; \mathbf{X} > \mathbf{R}^{1/2}\mathbf{Y}\mathbf{S}^{-1}\mathbf{Y}^{\mathrm{T}}\mathbf{R}^{1/2} \end{bmatrix} \tag{22}$$

where $\mathbf{X}$ is an auxiliary parameter. The inequality in (22) can be rewritten using the Schur complement formula (see Appendix)

$$\begin{bmatrix} \mathbf{X} & \mathbf{R}^{1/2}\mathbf{Y} \\ \mathbf{Y}^{\mathrm{T}}\mathbf{R}^{1/2} & \mathbf{S} \end{bmatrix} > 0 . \tag{23}$$

Therefore the problem (21) can be written as

$$\min_{\mathbf{Y},\,\mathbf{S},\,\mathbf{X}} \; Tr(\mathbf{Q}^{1/2}\mathbf{S}\mathbf{Q}^{1/2}) + Tr(\mathbf{X}) - Tr(\mathbf{Y}\mathbf{N}) - Tr(\mathbf{N}^{\mathrm{T}}\mathbf{Y}^{\mathrm{T}})$$

$$\text{subject to } \; \mathbf{A}\mathbf{S} - \mathbf{B}\mathbf{Y} + \mathbf{S}\mathbf{A}^{\mathrm{T}} - \mathbf{Y}^{\mathrm{T}}\mathbf{B}^{\mathrm{T}} + \mathbf{E}\mathbf{E}^{\mathrm{T}} < 0, \qquad \begin{bmatrix} \mathbf{X} & \mathbf{R}^{1/2}\mathbf{Y} \\ \mathbf{Y}^{\mathrm{T}}\mathbf{R}^{1/2} & \mathbf{S} \end{bmatrix} > 0, \qquad \mathbf{S} > 0 \tag{24}$$

Problem (24) is equivalent to the standard LQR problem defined by (14), and the feedback gain is then given by $\mathbf{K}_0 = \mathbf{F}_0 = \mathbf{Y}_0\mathbf{S}_0^{-1}$.

DISSIPATIVITY CONSTRAINTS

In this section, the dissipativity indices are investigated as candidates for a new inequality constraint to be appended to the EVP-LQR problem to induce higher levels of dissipativity.

Among the indices given, $D_{\%}$ cannot be represented in a manner suitable for the LQR problem since it is deterministic. To find a constraint for D_{p}, $\rho_{u_{\mathrm{a}}v_{\mathrm{d}}}$ is represented in a form suitable for the EVP first. Let the velocity of the system at the point where the damper exerts force be given by $v = \mathbf{C}_{\mathrm{v}}\mathbf{q}$. Since the LQR control force is a feedback force as $u_{\mathrm{a}} = -\mathbf{F}\mathbf{q}$, $\rho_{u_{\mathrm{a}}v_{\mathrm{d}}}$ can be written as

$$\rho_{u_{\mathrm{a}}v_{\mathrm{d}}} = \frac{E[-\mathbf{F}\mathbf{q}(\mathbf{C}_{\mathrm{v}}\mathbf{q})^{\mathrm{T}}]}{\sqrt{E[-\mathbf{F}\mathbf{q}(-\mathbf{F}\mathbf{q})^{\mathrm{T}}]}\sqrt{E[\mathbf{C}_{\mathrm{v}}\mathbf{q}(\mathbf{C}_{\mathrm{v}}\mathbf{q})^{\mathrm{T}}]}}. \tag{25}$$

Introducing the state covariance matrix $\mathbf{P} = E[\mathbf{q}\mathbf{q}^{\mathrm{T}}]$, a constraint for D_{p} is obtained as

$$\frac{1}{\pi}\operatorname{acos}\left(\frac{-\mathbf{F}\mathbf{P}\mathbf{C}_{\mathrm{v}}^{\mathrm{T}}}{\sqrt{\mathbf{F}\mathbf{P}\mathbf{F}^{\mathrm{T}}}\sqrt{\mathbf{C}_{\mathrm{v}}\mathbf{P}\mathbf{C}_{\mathrm{v}}^{\mathrm{T}}}}\right) > \gamma_{\mathrm{p}} \qquad \text{where} \quad 0 \le \gamma_{\mathrm{p}} \le 1. \tag{26}$$

Using the same notation, a constraint for D_{e} is found as

$$-\mathbf{F}\mathbf{P}\mathbf{C}_{\mathrm{v}}^{\mathrm{T}} < \gamma_{\mathrm{e}} \quad \text{where} \quad \gamma_{\mathrm{e}} < \mu_{\varepsilon}. \tag{27}$$

Similarly, a constraint for D_{ne} is given by

$$\frac{-\mathbf{F}\mathbf{P}\mathbf{C}_{\mathrm{v}}^{\mathrm{T}}}{\sqrt{\mathbf{F}\mathbf{P}\mathbf{F}^{\mathrm{T}}}\sqrt{\mathbf{C}_{\mathrm{v}}\mathbf{P}\mathbf{C}_{\mathrm{v}}^{\mathrm{T}}}} < \gamma_{\mathrm{ne}} \qquad \text{where} \quad -1 < \gamma_{\mathrm{ne}} < 1. \tag{28}$$

Clearly, the conditions given by

$$0.5 \le \gamma_{\mathrm{p}} \le 1, \qquad \gamma_{\mathrm{e}} < 0, \qquad -1 < \gamma_{\mathrm{ne}} < 0 \tag{29}$$

are more desired as the primary control force is more likely to dissipate energy for these values.

One should note that the normalized mean energy flow constraint given by (28) enforces the probability constraint (26) through a mapping, which can be visualized with the aid of Fig. 2. Since D_{ne} constraint (28) does not include a trigonometric function, it is more suitable for the EVP problem, and D_{p} constraint (26) is not considered further.

It is now required to find representations of the constraints given by (27) or (28) suitable for the EVP, *i.e.*, they should be representable in terms of Lyapunov matrices, $\mathbf{S}_{\mathrm{e}}$ and $\mathbf{S}_{\mathrm{ne}}$. However, the introduction of $\mathbf{S}_{\mathrm{e}}$ and $\mathbf{S}_{\mathrm{ne}}$ requires the addition of equality constraints given by

$$(\mathbf{A}-\mathbf{BF})\mathbf{S}_{\mathrm{e}} + \mathbf{S}_{\mathrm{e}}(\mathbf{A}-\mathbf{BF})^{\mathrm{T}} + \mathbf{E}\mathbf{E}^{\mathrm{T}} = 0 \quad \text{and} \quad (\mathbf{A}-\mathbf{BF})\mathbf{S}_{\mathrm{ne}} + \mathbf{S}_{\mathrm{ne}}(\mathbf{A}-\mathbf{BF})^{\mathrm{T}} + \mathbf{E}\mathbf{E}^{\mathrm{T}} = 0\,. \tag{30}$$

Moreover, since (28) is a nonlinear matrix inequality constraint, and a corresponding BMI and/or a LMI may not be available, a numerical solution of the EVP with the constraint (28) is not guaranteed by the available solution techniques. Therefore, substantial research may be required for the development of new techniques specific to (28) and (30) to obtain an at-least-local solution, which is out of the scope of this research. Therefore, the following constraint is used:

$$-\mathbf{F}\mathbf{S}\mathbf{C}_{\mathrm{v}}^{\mathrm{T}} < \gamma_{\mathrm{e}}^{\mathrm{L}} \quad \text{where} \quad \gamma_{\mathrm{e}}^{\mathrm{L}} < \mu_{\varepsilon}. \tag{31}$$

There are several advantages and disadvantages of this constraint. First of all, (31) does not fully represent the indices D_{e} and D_{ne} since the equality constraints (30) are dropped. Also, the term $-\mathbf{F}\mathbf{S}\mathbf{C}_{\mathrm{v}}^{\mathrm{T}}$ is not a normalized index. In contrast, this constraint simply allows a numerical solution to this sophisticated multiobjective problem, which is actually the fundamentally philosophy behind the LMI-EVP approach.

The dissipativity constraint (31) can be added to the LQR problem for various values of $\mu_{\varepsilon}^{\mathrm{L}}$. The new controllers may have various dissipativity levels and can be used in a semiactive system to investigate the correlation between the dissipativity indices and the performance.

NUMERICAL EXAMPLES

In this section, two numerical examples are investigated to understand how dissipativity characteristics of a semiactive system are related to its performance. The first example is a simple two-degree-of-freedom shear structure where an ideal smart damper is placed in the first story. The second example is a simple highway bridge model with a rubber bearing and an MR damper between the superstructure and the sub-

structure. For each example, the structural parameters are explained first. Then, the EVP problem (20) is verified to be equivalent to the corresponding LQR problem using a simple control design. Finally, for each example, a set of LQR controller parameters is defined, and the structural system is analyzed numerically for white noise excitations, with or without the dissipativity constraint (31). The performance and dissipativity characteristics are presented graphically. The control systems investigated for the 2DOF building and bridge models are summarized in Table 1 and as follows:

- *Act*: This is a theoretical fully active system. A fictitious fully active actuator is used instead of a smart damper. Standard LQR is used to command the actuator.
- *Act-Dis*: This system is also a theoretical fully active system. A fictitious fully active actuator is used instead of a smart damper. The proposed LMI-EVP controller with the dissipativity constraint is utilized instead of the standard LQR to observe how the added dissipativity constraint changes the dissipative nature of the active control force.
- *SAct*: This is a semiactive system where a smart damper is used. A clipped optimal control strategy is utilized to command the smart damper. The primary controller in the clipped optimal control is a standard LQR controller.
- *SAct-Dis*: This is also a semiactive system where a smart damper is used. A clipped optimal control strategy is utilized to command the smart damper. The primary controller in the clipped optimal control is the proposed LMI-EVP controller with the dissipativity constraint.

TABLE 1 A summary of the systems analyzed in the numerical examples.

Systems	Control Device	Control Strategy	Primary Controller	$-\mathbf{FSC}_v^T < \gamma_e^L$
Act	Fully Active	LQR	—	Not Incl.
Act-Dis	Fully Active	LMI-EVP	—	Included
SAct	Smart Damper	Clipped Opt.	LQR	Not Incl.
SAct-Dis	Smart Damper	Clipped Opt.	LMI-EVP	Included

Numerical Example: A 2DOF Building Structure

The 2DOF shear building model shown in Fig. 3 is considered as the first numerical example. The equation of motion and the state-space representation of the equation of motion are straightforward and will not be given here. The floor masses m_1 and m_2

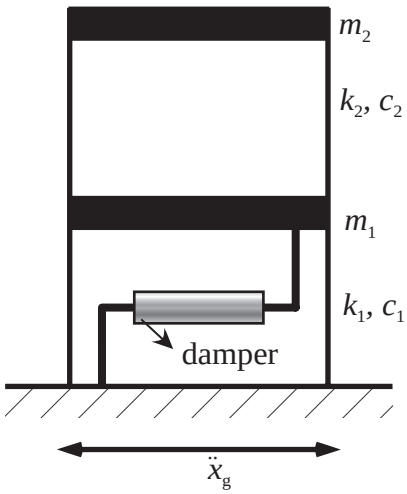

FIG. 3 The two-DOF system.

are 100 tons. The stiffnesses k_1 and k_2 are selected such that the story periods are 0.5 secs. Similarly, the floor damping coefficients are found by setting the modal damping ratios to 2%. An ideal smart damper is attached between the first floor and the ground.

An ideal damper can be considered as an active actuator that can only apply dissipative forces, *i.e.,* forces that are strictly dissipative. Therefore, in the clipped optimal control strategy, an ideal damper can successfully mimic the primary controller when the primary controller force is strictly dissipative; otherwise, it produces no force. This behavior can be characterized as follows:

$$u_{\mathrm{d}} = \begin{cases} u_{\mathrm{a}}, & u_{\mathrm{a}} v_{\mathrm{d}} < 0 \\ 0, & u_{\mathrm{a}} v_{\mathrm{d}} \geq 0 \end{cases} \tag{32}$$

where u_{d} and v_{d} are the damper force and velocity, respectively, and u_{a} is the primary control force.

The equivalency of the LQR problem and the LMI-EVP are verified for a set of design parameters given by

$$\mathbf{Q} = \begin{bmatrix} \mathbf{K} & \mathbf{0} \\ \mathbf{0} & \mathbf{M} \end{bmatrix} \qquad \mathbf{R} = 10^{-4}\ \mathrm{m/N} \qquad \mathbf{N} = [1 \quad 1 \quad 1\mathrm{s} \quad 1\mathrm{s}]^{\mathrm{T}}. \tag{33}$$

which satisfies the positive definite inequality (17). Note that the dissipativity constraint is not employed here. It is found that the gains and covariance matrices obtained from LQR and LMI approaches are identical within numerical round-off accuracy. Also, other weighting matrix sets that satisfy the positive definite inequality (17) are observed to give identical gains and covariances, whereas those not satisfying (17) give different results as the LQR optimization problem is then improper. It is also observed that both approaches give different results for some control designs, even though inequality (17) is satisfied; for these designs, it is found that the smallest eigenvalue of $\mathbf{W}$ in (17) is very close to zero, *e.g.* $o(10^{-10})$, which causes numerical problems in the solution methods.

Having verified the LMI-LQR equivalency, a new control design is introduced to be used in the dissipativity analysis. The output vector to be minimized is selected as the drifts of each story and the absolute accelerations of each floor, $\mathbf{z} = [x_1 \quad x_2 - x_1 \quad \ddot{x}_1^{\mathrm{abs}} \quad \ddot{x}_2^{\mathrm{abs}}]^{\mathrm{T}}$. The control design parameters are selected as

$$\tilde{\mathbf{Q}} = \begin{bmatrix} \alpha \mathbf{I}_{2\times 2} & \mathbf{0} \\ \mathbf{0} & \dfrac{\beta}{\omega_{\mathrm{n}}^4} \mathbf{I}_{2\times 2} \end{bmatrix} \qquad \tilde{\mathbf{R}} = \eta \qquad \tilde{\mathbf{N}} = \mathbf{0}. \tag{34}$$

This set of parameters allows one to choose the relative importance of the drift and absolute acceleration responses. The normalization frequency ω_{n} is taken as a $10.5\,\mathrm{rad/sec}$; this value is found such that the drift and absolute acceleration portions of the term $E[\mathbf{z}^{\mathrm{T}}\tilde{\mathbf{Q}}\mathbf{z}]$ give the same values for ($\alpha = 1$, $\beta = 1$) in active control.

As a first attempt, a MATLAB code is written where the dissipativity constraint (31) with several values of $\gamma_{\mathrm{e}}^{\mathrm{L}}$ is simply appended to the LMI-EVP to obtain the smallest possible value of D_{e} for a given set of control design parameters. During this initial study, it is found that one of the parameters of the MATLAB LMI solver, known as feasibility radius R_{f}, affects the results considerably. R_{f} creates a limit for the Euclidian magnitude of the EVP parameter $\mathbf{x}$ (see inequality (9) above) for numerical efficiency. It is observed that for a given $\gamma_{\mathrm{e}}^{\mathrm{L}}$, different values of the feasibility radius yield different dissipativity levels. This is a natural consequence of the dissipativity constraint (31), which includes a term that is not normalized. Therefore, a parametric study is carried out to find the $(\gamma_{\mathrm{e}}^{\mathrm{L}}, R_{\mathrm{f}})$ pair that yields the smallest D_{e} for each control design. The resulting $(\gamma_{\mathrm{e}}^{\mathrm{L}}, R_{\mathrm{f}})$ values are then employed in the dynamic analysis of the 2DOF structure excited by an artificial white noise signal for the corresponding control designs. The performance of the structure is investigated using three indices given by

$$J_{\mathrm{d}} = \sigma_{x_1}^2 + \sigma_{x_2 - x_1}^2 \tag{35}$$

$$J_{\mathrm{a}} = \frac{1}{\omega_{\mathrm{n}}^4}(\sigma_{\ddot{x}_1^{\mathrm{abs}}}^2 + \sigma_{\ddot{x}_2^{\mathrm{abs}}}^2) \tag{36}$$

$$J = J_{\mathrm{d}} + \frac{\beta}{\alpha}J_{\mathrm{a}} + \frac{\eta}{\alpha}\sigma_{\mathrm{u}}^2 . \tag{37}$$

where, for a discrete time history $x(n\Delta t)$, σ_x^2 is defined by

$$\sigma_x^2 = \frac{1}{N}\sum_{k=1}^{N}[x(k\Delta t)]^2 . \tag{38}$$

The following results are obtained for $\beta = 1000$ and several values of α ranging from 10^{-5} to 10^{5}.

Fig. 4 shows the dissipativity characteristics of the controllers for the 2DOF building structure, where the terms D_{n} and D_{ne} are obtained using stochastic analysis for a white noise excitation with an intensity $1/100$ (see the explanation for Fig. 5). Fig. 5 shows $D_{\%}$ and J plots where the structure is excited with a 100 sec white noise signal. It is observed that the peak acceleration of the generated white noise signal is

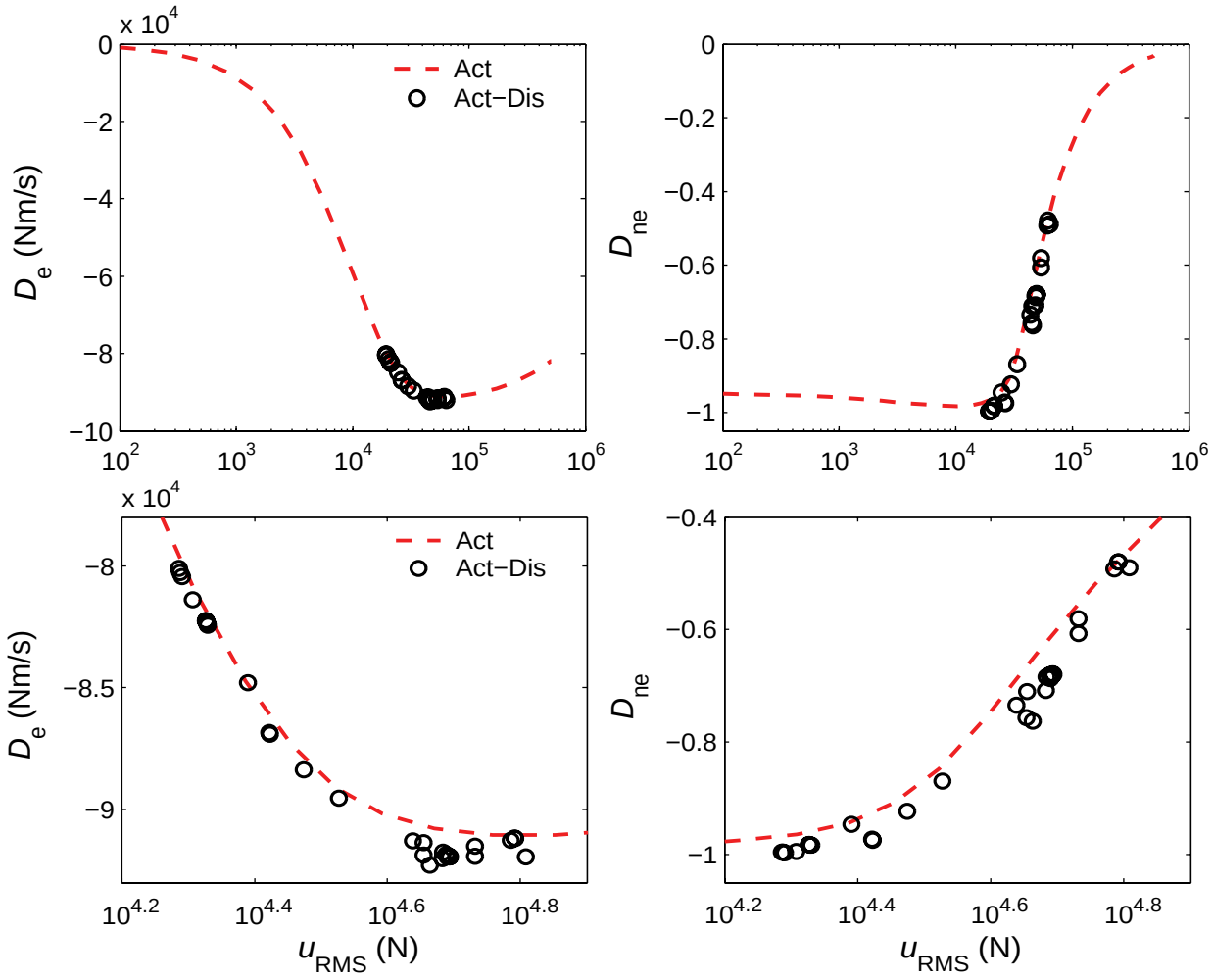

FIG. 4 D_{n} and D_{ne} plots for the 2DOF building structure from the covariance analysis (overall and detailed).

around 50 m/s^2. Therefore, the white noise is normalized by a factor of 10 to have an excitation that is consistent with the well known historical earthquake ground acceleration data. Note that the results of the covariance analyses, which is given by Fig. 4 is also normalized accordingly. Fig. 6 shows the displacement and acceleration indices for the semiactive systems. In all of the above plots, the performance indices are normalized with the corresponding uncontrolled system indices. Note that the control force term in the index J is not used for the uncontrolled structure. The following observations are made:

- For practical control force levels ($[10^4, 10^5]$ N in Fig. 5) the dissipativity of the controller is very high for this particular structure and control design.
- It is observed that the variation of D_{e} is not similar to the variation of D_{ne} for the active system (Act), *i.e.*, for small control force levels D_{e} is low while D_{ne} is high. This difference can be attributed to the

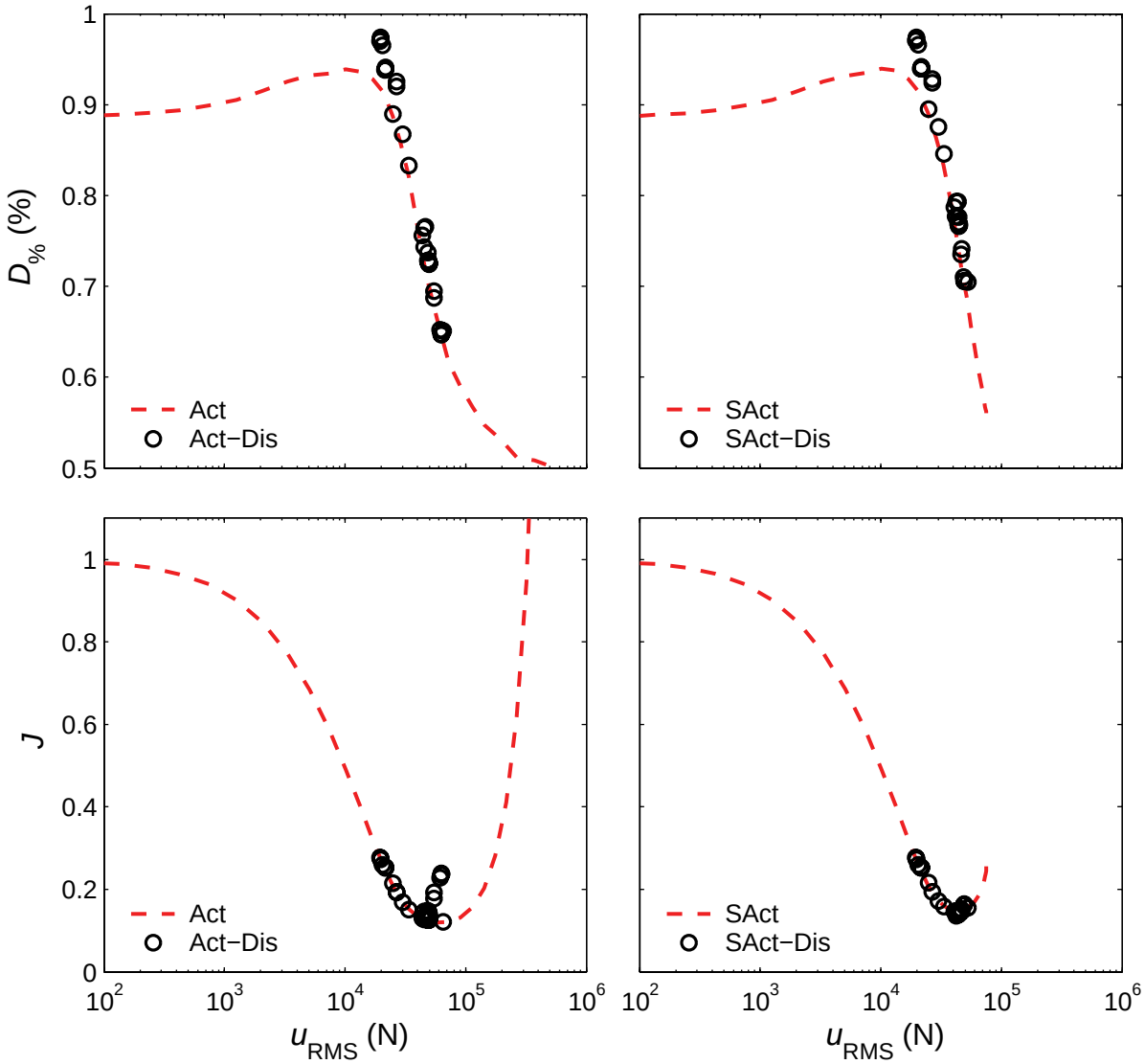

FIG. 5 $D_{\%}$ and normalized J plots for the 2DOF building structure from the simulations for a white noise excitation.

magnitudes of the RMS control force and RMS velocity used as normalization coefficients in the computation of D_{ne}. Therefore, although a high value of D_{ne} indicates highly dissipative control forces, the corresponding control design may not be suitable for practical purposes due to low control force levels.

- The LMI method improves D_e and D_{ne} for a given u_{RMS}. This is more clear for $u_{RMS} \approx 10^{4.65}$ N. However, the best improvement in $D_{\%}$ is for $u_{RMS} \approx 10^{4.2}$ N. Moreover, it is observed that the LMI method improves the drift performance about 25% for $u_{RMS} \approx 10^{4.65}$ N. This improvement is not clear on the overall performance index J.

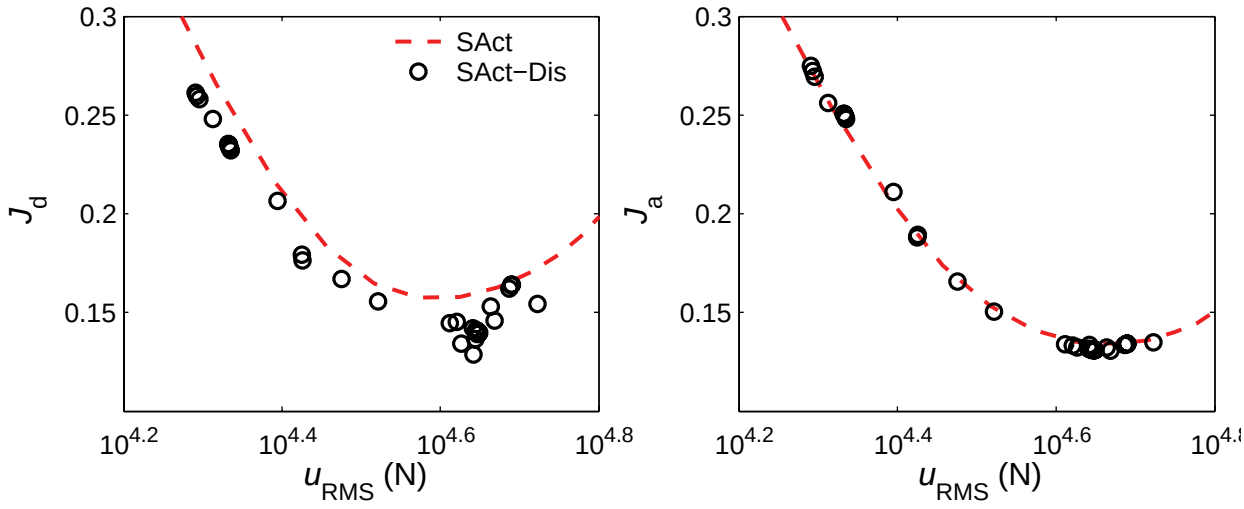

FIG. 6 Detailed plots of normalized J_d and J_a of the 2DOF building structure from the simulations for a white noise excitation.

- Another difference between D_e and D_{ne} is that the highest value of D_e corresponds to RMS control force levels of $[10^{4.6}, 10^{4.8}]$ N, while this range is $[10^{4.2}, 10^{4.4}]$ N for D_{ne}. Also observed is the similarity between D_{ne} and $D_{\%}$ (note that the $D_{\%}$ plot should be flipped vertically to visualize this similarity).
- The LMI method narrows the range of possible u_{RMS} values for the control designs. This is a very useful property in the design process. In general, one must do a comprehensive parametric study, which may include computationaly expensive nonlinear analyses, to find the best (α, β) pair for a given η. The LMI method and the dissipativity indices may give a good sense of the achievable semiactive performance letting the designer to avoid simulations that will not yield better results.
- The plot of overall performance index shows a high similarity to the D_e plot. Therefore, for this example, D_e is more useful to guess the best control design.

The indices given in this paper are very helpful to understand the dissipative nature of the primary control force and the semiactive performance of this example. The LMI method is able to modify the dissipativity characteristics of the controller so that the semiactive performance is improved. Two critical designs are located. The first design corresponds to $u_{RMS} \approx 10^{4.2}$ N, and the LMI method improves the indices D_{ne} and $D_{\%}$ though it is not the best semiactive design. The second design point is for $u_{RMS} \approx 10^{4.65}$ N, which has the best semiactive performance and the highest improvement in D_e. The results for these two designs are summarized in Tables 2 and 3. Therefore, each index shows different characteristics of the control force and may be useful to understand different problems.

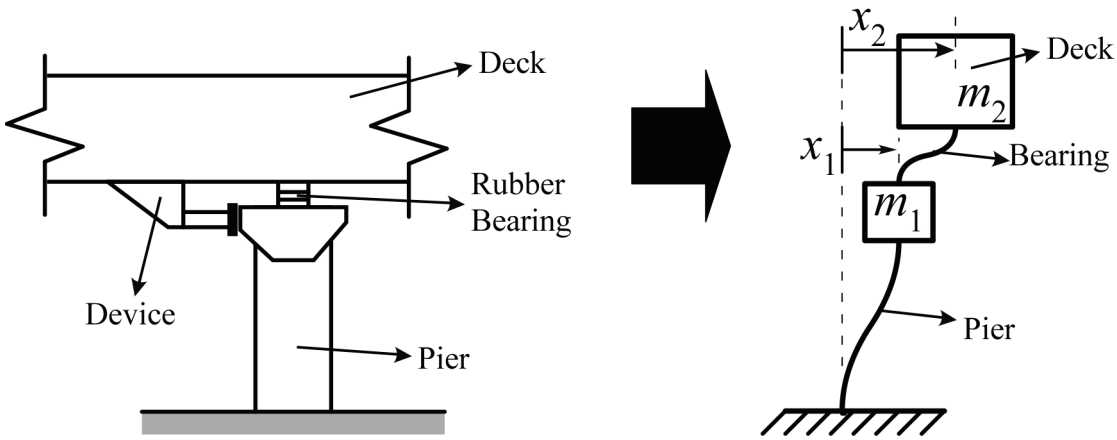

FIG. 7 2DOF modelling of the highway bridge (Erkus *et al*. 2002)

Numerical Example: 2DOF Highway Bridge Model

The bridge model shown in Fig. 7 is used as the second example. In this model, the mass ratio, damping ratio and natural period of the pier are $m_2/m_1 = 5$, 5% and 0.5 sec, respectively. The mass of the pier is $m_1 = 100$ ton. The bearing stiffness is 7.685×10^6 N/m, which is computed using a formula for opti-

TABLE 2 Indices for design $u_{\mathrm{RMS}} \approx 10^{4.2}$ N

	D_{n} (Nm/s)	D_{ne}	$D_{\%}$ (%)	J_{d}	J_{a}
Act	-7.983×10^4	–0.966	0.917	-	-
Act-Dis	-8.043×10^4	–0.997[a]	0.974[a]	-	-
SAct	-	-	0.917	0.283	0.273
SAct-Dis	-	-	0.974[a]	0.258	0.269

a. Highest dissipativity achieved.

TABLE 3 Indices for design $u_{\mathrm{RMS}} \approx 10^{4.8}$ N

	D_{n} (Nm/s)	D_{ne}	$D_{\%}$ (%)	J_{d}	J_{a}
Act	-9.073×10^4	–0.652	0.721	-	-
Act-Dis	-9.229×10^4 [a]	–0.763	0.765	-	-
SAct	-	-	0.760	0.160	0.135
SAct-Dis	-	-	0.793	0.129[b]	0.134

a. Highest dissipativity achieved.
b. Highest performance achieved.

mal stiffness (Erkus *et al*. 2002). For active control, the damping of the bearing is assumed to be zero and for the uncontrolled structure it is taken as 196 kN·s/m. If the design goal is to reduce the pier response where a damper is attached between the pier and the deck, a particular control design may yield low dissipativity levels, and the damper cannot mimic the primary control force efficiently (Erkus *et al*. 2002). Note that this dissipativity characteristic is also observed by Inaudi (2000) by an analytical study. The mathematical model is already given by Erkus *et al*. (2002) and will not be repeated here. The damper in the original paper (Erkus *et al*. 2002) is an MR fluid damper and a mathematical model of a prototype small-scale MR fluid damper is used in the analysis. This study, however uses a more realistic damper model, which is obtained for a 20-ton MR fluid damper. The details of this new model are given by Yang *et al*. (2002). In the analysis, the damper force is amplified by a factor of 3 to be able to exert forces commanded by the primary control force (in a practical application a 60-ton damper would be used). The equivalency of the LMI-EVP and LQR problem is tested for this example using several control design parameters. It is found that the two methods yield identical results when the dissipativity constraint is not employed and condition (17) is satisfied.

In this example, $\mathbf{R} = 10^{-12}$ N·m and the control design parameter $\mathbf{Q}$ is selected such that the term $\mathbf{q}^{\mathrm{T}}\mathbf{Q}\mathbf{q}$ represents an energy quantity *i.e.*,

$$\mathbf{q}^{\mathrm{T}}\mathbf{Q}\mathbf{q} = r\left(\frac{1}{2}k_1(x_1)^2 + \frac{1}{2}m_1(v_1)^2\right) + \left(\frac{1}{2}k_1(x_2 - x_1)^2 + \frac{1}{2}m_1(v_2 - v_1)^2\right) \tag{39}$$

where r determines the relative importance of the pier and the bearing responses. In this example, $r = 1000$ is selected, which results in LQR controllers with low dissipativity levels. Using this particular controller design, the LMI-EVP problem is solved for several values of $\gamma_{\mathrm{e}}^{\mathrm{L}}$ to increase the controller dissipativity. After some test simulations, $R_{\mathrm{f}} = 1 \times 10^{30}$ is used. The results are plotted for $\gamma_{\mathrm{c}} = -\gamma_{\mathrm{e}}^{\mathrm{L}} / R_{\mathrm{f}}$.

Fig. 8 shows the dissipativity and performance characteristics of the LMI-EVP controller for various values of $\gamma_{\mathrm{e}}^{\mathrm{L}}$, which is obtained by standard stochastic analysis. In these plots, the values are normalized by the corresponding standard LQR controller values. Fig. 9 shows the dissipativity nature of the controllers and performance of the systems for both active and semiactive systems excited by the white noise signal used in the first example. In these plots, the RMS response values are normalized by the corresponding RMS values of an uncontrolled structure given by Erkus *et al*. (2002), and the maximum control force values are normalized by the total weight of the structure. The followings are observed:

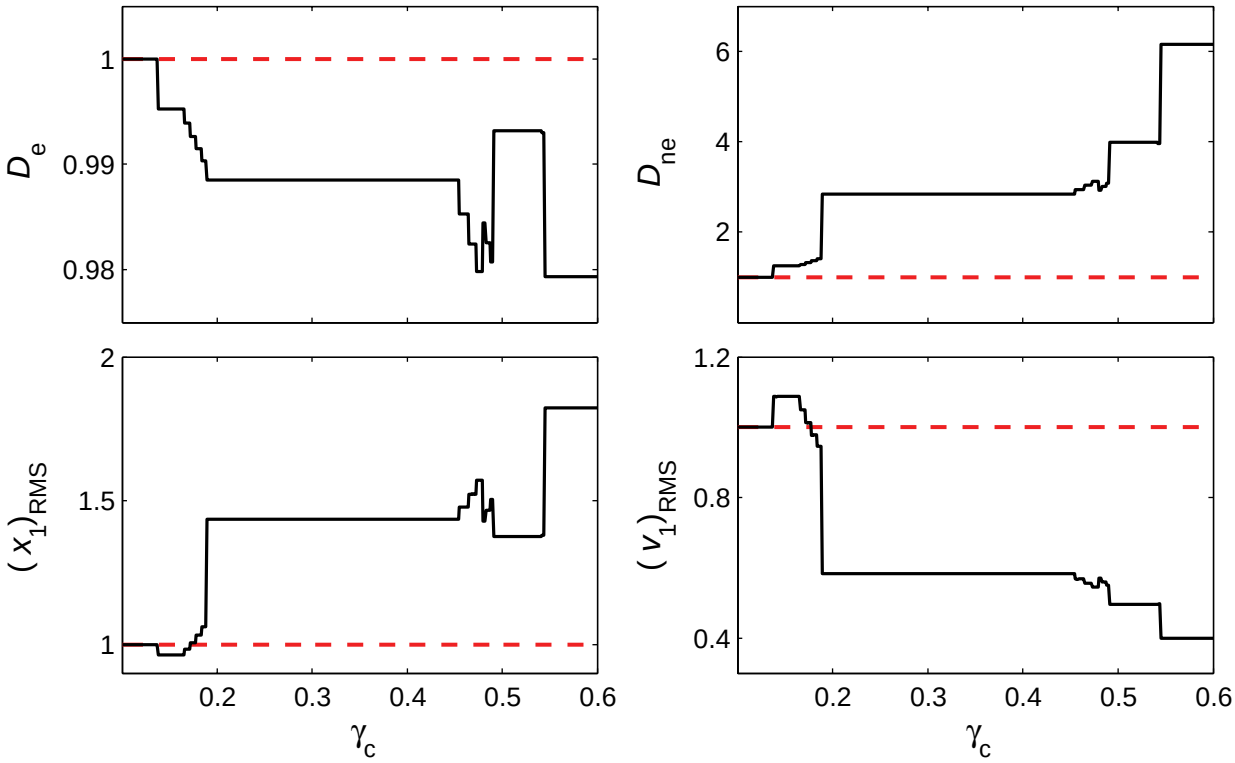

FIG. 8 Normalized D_e, D_{ne} and performance plots of the LMI-EVP controller of the 2DOF bridge structure for various γ_e^L values (covariance analysis).

- As seen in Fig. 8, the LMI method improves the dissipativity index D_{ne} even though the weak form of the dissipativity constraint is used. On the other hand, the index D_e indicates a reduction in the mean energy flow rate. It is also observed that there is an improvement in the drift index for $\gamma_c \approx 0.15$ although this is not anticipated. In the design process, this point may be considered more suitable for a semiactive design.

- The simulation results given in Fig. 9 show that improving dissipativity characteristics makes a very minor improvement on the semiactive drift performance. There are several reasons for this result. First, Act-Dis performance does not improve; indeed, $(x_1)_{RMS}$ increases considerably. Second, the damper is not an ideal damper and has a very nonlinear dynamics. It is not as efficient as an ideal damper in applying the required force.

- A more interesting observation that effects the semiactive performance is that the dissipativity index $D_{\%} \approx 52\%$ of the active system reduces to $D_{\%} \approx 25\%$ for the semiactive system. The main reason for this reduction is inability of the MR damper to apply nondissipative forces. The active controller with

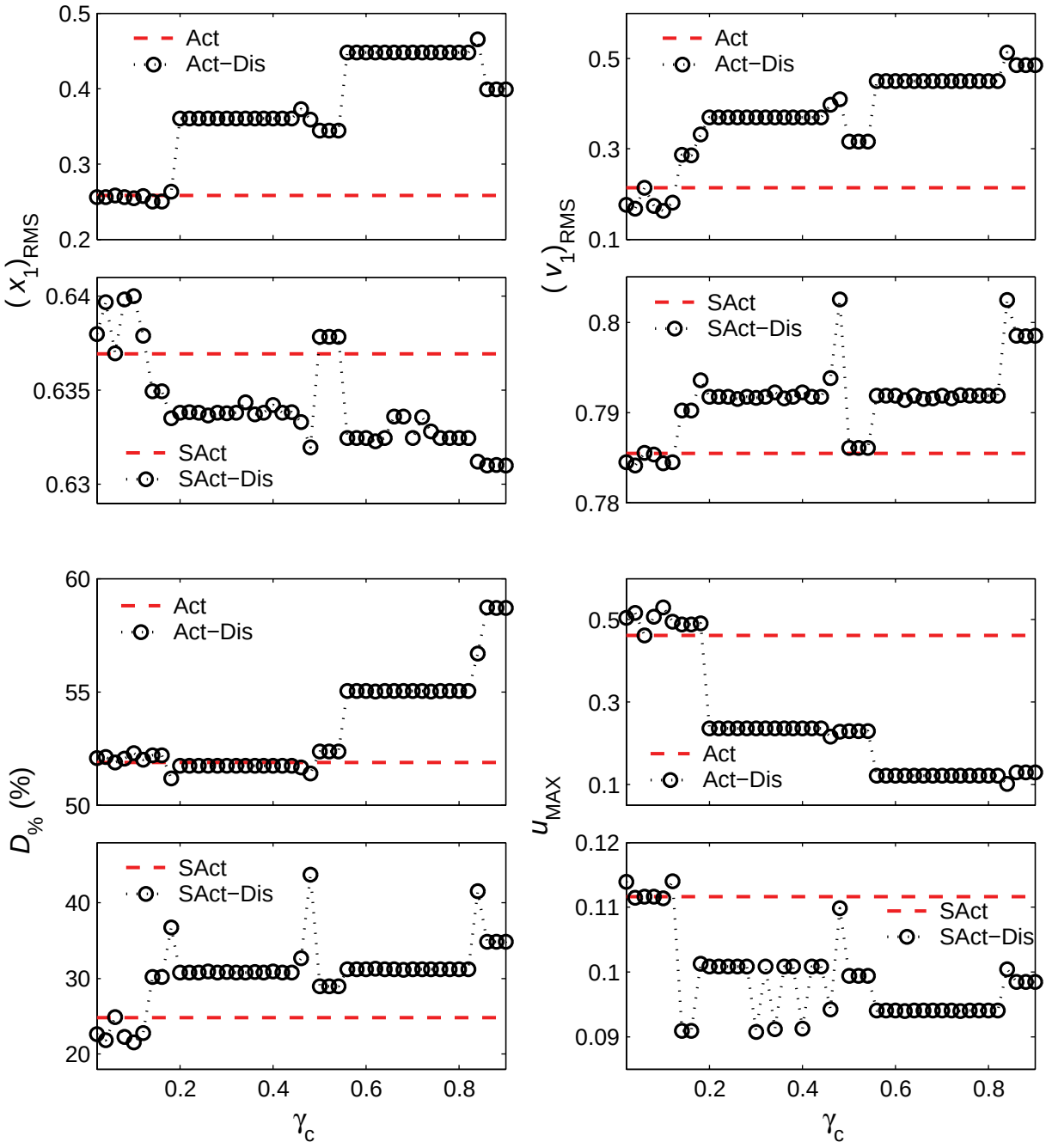

FIG. 9 Normalized $D_{\%}$ and normalized performance plots for the 2DOF bridge structure from the simulations for a white noise excitation.

$D_{\%} \approx 52\%$ requires nondissipative forces, probably ones that inject energy into the structural system. During the simulation, the damper will not be able to mimic the active control force since it cannot exert nondissipative forces. Therefore, the response of the semiactive system will be considerably different from a corresponding fully active system response. In this case, the primary controller (standard

LQR) will command forces that inject even more energy than in the active case to push back the semiactive response path into the fully active response path. This will yield control forces with even lower dissipativity than expected. Obviously, if an ideal damper model were used, this effect will not be as significant as in the MR fluid damper case. Therefore, it can be concluded that the use of semiactive devices to implement very nondissipative control designs may reduce the semiactive performance in two ways: first, performance reduction due to low dissipativity; second, additional dissipativity reduction due to the inability of the damper to mimic a nondissipative control force.

- Although the LMI approach improves the dissipativity, it cannot compensate for the severe reduction caused by the damper effect described above, and its benefits are not observed on the final semiactive performance.

- The benefit of improved dissipativity is the lowered control force levels implemented by the damper. About 20% reduction occurred on the maximum control force required for $\gamma_c = (0.6, 0.8)$ to achieve the same drift performance. It should be noted that there may be other control design parameter sets that gives the same performance improvement, though a comprehensive and time consuming parametric study would be required to search for the existence of such sets. On the other hand, the proposed LMI method allows one to achieve the same performance without an extensive and time consuming study.

CONCLUSIONS

In this paper, the dissipativity and performance of semiactive systems with smart dampers are investigated. In addition to a brief review of previously defined dissipativity indices, two new indices are defined. For this purpose, a formal definition of a strictly dissipative force is introduced, and dissipativity indices are defined for the primary control force in a clipped optimal control strategy. The statistical and physical relations among these dissipativity indices are discussed. Then, a method based on LMI control design is proposed to modify the dissipativity characteristics of the primary control force. The method converts an LQR problem into a multiobjective EVP form where new inequality constraints can be imposed on the controller. Based on the indices defined, possible inequality constraints are derived. It is found that, due to the nature of the EVP, only a weak constraint can be used to modify the EVP. This constraint is then employed for two numerical examples: a highly dissipative control design for a 2DOF frame structure with an ideal damper and a minimally dissipativity control design for a 2DOF model of an elevated highway

bridge with a realistic MR fluid damper model. In the first example, the dissipativity indices were very useful for understanding different characteristics of the controller, and the proposed LMI approach was able to considerably improve drift performance of the controller. In the second example, although the LMI method was able to improve the dissipative nature of the primary controller, this improvement was not reflected in the final semiactive performance efficiently since the use of a realistic damper model with a nondissipative primary controller lowers the original dissipativity. In summary, the dissipativity indices are useful for understanding the performance of a semiactive system with a smart damper, and the proposed LMI method proposed is able to modify the dissipativity levels of the controller even though a weak form of the dissipativity constraint is employed.

ACKNOWLEDGEMENTS

The authors gratefully acknowledge the partial support of this research by the National Science Foundation under CAREER grant CMS 00-94030, and by the U.S. Department of Transportation through grant 03-17 from the National Center for Metropolitan Transportation Research (METRANS).

APPENDIX I. RELEVANT LITERATURE

In this section, a literature survey relevant to the concepts presented in this paper are given.

Dissipativity and Dissipative Systems

There are several definitions of dissipativity in the field of systems and control. In fact, dissipativity is one of the key concepts in control theory, and there is a vast body of literature regarding dissipative systems. However, one should note that these definitions are used to characterize input–output relations of dynamic systems and that these are different from the mechanical definition used herein. Rather, dissipativity is associated with the control force, and the concept of dissipative force is introduced based on mechanical energy dissipation of energy in this study. Although a connection between these two interpretations can be found, this is beyond the scope of this paper. Interested readers are directed to the works by Gurtin and Herrera (1964), Willems (1972a,b), Taylor (1974), Ioannou and Tao (1987) and Wen (1988) for further details.

Convex Multiobjective Optimization via LMIs

Convex optimization techniques became very popular in the control field since it has been shown that important control problems, such as robust H_2 and H_∞ control problems, can be represented in terms of LMIs. These techniques allow numerical solution of complex problems with multiobjective goals that have no analytical solution. In fact, the LQR problem defined herein can be represented as an H_2 problem, and available an LMI representation of an H_2 problem can be used. However, robust H_2 control theory is quite involved and requires a good knowledge of frequency and time domain analysis. In contrast, LQR is well known and widely applied within the structural control community; therefore, LQR is used herein. Interested readers are directed to the works by Willems (1971), Khargonekar and Rotea (1991), Feron *et al*. (1992), Peres *et al.* (1992), Boyd *et al*. (1994), Safonov *et al*. (1994), Scherer *et al*. (1997), Turan *et al*. (1997), Masubuchi *et al*. (1998), and Dullerud and Paganini (2000) for further details. Application of LMI techniques to structural control problems is very recent. Some examples are Yang *et al*. (2003) and Yang *et al*. (2004).

APPENDIX II. DEFINITIONS AND THEOREMS

In this section, some essential definitions and theorems are given.

Definition A.1 A function $f(x)$ is a *linear* function of x if $f(\alpha x_1 + \beta x_2) = \alpha f(x_1) + \beta f(x_2)$ for all scalar α and β.

Definition A.2 A function $g(x)$ is an *affine* function of x if it can be written as $g(x) = f(x) + a$ where $f(x)$ is a linear function and a is a constant.

According to the definitions given above, all linear functions are affine but not all affine functions are linear. For example, the function $\mathbf{F}(\mathbf{x})$ given in (10) is an affine function of $\mathbf{x}$, not linear. Some authors (*e.g*., Dullerud and Paganini 2000) prefer to use the following for the definition of an LMI:

$$\mathbf{F}(\mathbf{x}) = x_1\mathbf{F}_1 + \ldots + x_n\mathbf{F}_n > -\mathbf{F}_0 . \tag{A.1}$$

where $\mathbf{F}(\mathbf{x})$ is a linear function of $\mathbf{x}$.

Definition A.3 A set $C \subset \Re^n$ is *convex* if $\mu\mathbf{x}_1 + (1-\mu)\mathbf{x}_2 \in C$ for any $\mathbf{x}_1, \mathbf{x}_2 \in C$ and any $\mu \in [0, 1]$.

Theorem A.1 (*Schur complement formula*) The set of matrix inequalities

$$\mathbf{R} > 0 \quad \text{and} \quad \mathbf{Q} - \mathbf{S}\mathbf{R}^{-1}\mathbf{S}^{\mathrm{T}} > 0 \tag{A.2}$$

is equivalent to

$$\begin{bmatrix} \mathbf{Q} & \mathbf{S} \\ \mathbf{S}^{\mathrm{T}} & \mathbf{R} \end{bmatrix} > 0 \quad \text{and} \quad \mathbf{R} > 0 \tag{A.3}$$

where $\mathbf{Q}$, $\mathbf{R}$ and $\mathbf{S}$ are matrices, and $\mathbf{Q}$ and $\mathbf{R}$ are symmetric. See Dullerud and Paganini (2000) for a proof.

Definition A.4 The inequality $\mathbf{F}(\mathbf{x}) \geq 0$ is a *nonstrict* LMI while $\mathbf{F}(\mathbf{x}) > 0$ is a *strict* LMI.

From an engineering and computational point of view, a strict LMI is not different from its nonstrict version. For example, the dissipativity constraint is herein represented as a strict LMI in numerical computations for consistency. However, there are also situations where the computations are quite sensitive to the inequality condition. For example, during numerical simulations, it is observed that, for some specific values of the weighting matrices, the corresponding LQR problem turns out to be ill-conditioned even though the conditions for the well-posedness given by (17) are satisfied. It is found that some of the eigenvalues of $\mathbf{W}$ are very close to zero (in the range of 10^{-10}) for these weighting matrices. Therefore, it is highly recommended that the LQR weighting matrices be selected such that the smallest eigenvalue of $\mathbf{W}$ is large enough to guarantee the well-posedness of the LQR.

Next, the equivalency of the problems given by (19) and (20) is proven. For this purpose, some useful corollaries are given first. In corollaries (A.2) to (A.6), it is assumed that $\mathbf{S} = \mathbf{S}^{\mathrm{T}} > 0$, $\mathbf{P} = \mathbf{P}^{\mathrm{T}} > 0$ and $\mathbf{A}$ is Hurwitz. Also, the following shorthand notations are used: $\mathbf{L}_{\mathbf{S}} \equiv \mathbf{A}\mathbf{S} + \mathbf{S}\mathbf{A}^{\mathrm{T}} + \Psi$ and $\mathbf{L}_{\mathbf{P}} \equiv \mathbf{A}\mathbf{P} + \mathbf{P}\mathbf{A}^{\mathrm{T}} + \Psi$ where $\Psi = \Psi^{\mathrm{T}} > 0$.

Corollary A.2 $\mathbf{S} > \mathbf{P} \Leftrightarrow \mathbf{L}_{\mathbf{S}} < \mathbf{L}_{\mathbf{P}}$.

Proof: $\mathbf{S} > \mathbf{P} \Leftrightarrow \mathbf{S} - \mathbf{P} > 0 \Leftrightarrow \mathbf{A}(\mathbf{S} - \mathbf{P}) + (\mathbf{S} - \mathbf{P})\mathbf{A}^{\mathrm{T}} < 0 \Leftrightarrow \mathbf{A}\mathbf{S} + \mathbf{S}\mathbf{A}^{\mathrm{T}} < \mathbf{A}\mathbf{P} + \mathbf{P}\mathbf{A}^{\mathrm{T}} \Leftrightarrow \mathbf{L}_{\mathbf{S}} < \mathbf{L}_{\mathbf{P}}$.

Corollary A.3 $\mathbf{L}_{\mathbf{S}} < 0$ and $\mathbf{L}_{\mathbf{P}} = \mathbf{0} \Rightarrow \mathbf{S} > \mathbf{P}$. This is a consequence of corollary A.2.

Corollary A.4 $\Phi = \Phi^{\mathrm{T}} > 0 \Rightarrow Tr(\mathbf{C}\Phi\mathbf{C}^{\mathrm{T}}) > 0$.

Proof: Let $\mathbf{c}_i$ be the i^{th} row of $\mathbf{C}$. Then, $\Phi > 0 \Leftrightarrow \mathbf{c}_i\Phi\mathbf{c}_i^{\mathrm{T}} > 0 \ \forall i \Rightarrow \sum_i \mathbf{c}_i\Phi\mathbf{c}_i^{\mathrm{T}} = Tr(\mathbf{C}\Phi\mathbf{C}^{\mathrm{T}}) > 0$.

Corollary A.5 $\mathbf{S} > \mathbf{P} \Rightarrow Tr(\mathbf{C}\mathbf{S}\mathbf{C}^{\mathrm{T}}) > Tr(\mathbf{C}\mathbf{P}\mathbf{C}^{\mathrm{T}})$.

Proof: $\mathbf{S} > \mathbf{P} \Leftrightarrow \mathbf{S} - \mathbf{P} > 0 \Rightarrow Tr[\mathbf{C}(\mathbf{S}-\mathbf{P})\mathbf{C}^{\mathrm{T}}] > 0 \Leftrightarrow Tr(\mathbf{C}\mathbf{S}\mathbf{C}^{\mathrm{T}} - \mathbf{C}\mathbf{P}\mathbf{C}^{\mathrm{T}}) > 0 \Leftrightarrow Tr(\mathbf{C}\mathbf{S}\mathbf{C}^{\mathrm{T}}) - Tr(\mathbf{C}\mathbf{P}\mathbf{C}^{\mathrm{T}}) > 0 \Leftrightarrow Tr(\mathbf{C}\mathbf{S}\mathbf{C}^{\mathrm{T}}) > Tr(\mathbf{C}\mathbf{P}\mathbf{C}^{\mathrm{T}})$.

Corollary A.6 Let $S = \{\mathbf{S} | \mathbf{L}_{\mathbf{S}} < 0\}$, Then, there exists a unique matrix $\mathbf{P}_0$ such that $\mathbf{P}_0 = [\mathbf{P} | \mathbf{L}_{\mathbf{P}} = 0]$ and $\mathbf{P}_0 < \mathbf{S}$ for any $\mathbf{S} \in S$. Moreover, $Tr(\mathbf{C}\mathbf{P}_0\mathbf{C}^{\mathrm{T}}) < Tr(\mathbf{C}\mathbf{S}\mathbf{C}^{\mathrm{T}})$ holds for any $\mathbf{S} \in S$.

Proof: See corollaries A.3 and A.5.

Lemma A.7 Let

$$\mathbf{S}_0 = \arg \min_{\mathbf{S}} \; Tr(\mathbf{C}\mathbf{S}\mathbf{C}^{\mathrm{T}}) \quad \text{subject to} \quad \mathbf{L}_{\mathbf{S}} \le 0 \qquad \text{and} \qquad \mathbf{P}_0 = [\mathbf{P} | \mathbf{L}_{\mathbf{P}} = 0]. \tag{A.4}$$

Then, $\mathbf{S}_0 = \mathbf{P}_0$ and $Tr(\mathbf{C}\mathbf{S}_0\mathbf{C}^{\mathrm{T}}) = Tr(\mathbf{C}\mathbf{P}_0\mathbf{C}^{\mathrm{T}})$. The proof is readily obtained using corollary A.6.

Theorem A.8 The problems given by (19) and (20) are equivalent.

Proof: It can be shown with some matrix algebra that the objective function in the LQR problem can be written as

$$Tr(\mathbf{Q}^{1/2}\mathbf{P}\mathbf{Q}^{1/2}) + Tr(\mathbf{R}^{1/2}\mathbf{K}\mathbf{P}\mathbf{K}^{\mathrm{T}}\mathbf{R}^{1/2}) - Tr(\mathbf{K}\mathbf{P}\mathbf{N}) - Tr(\mathbf{N}^{\mathrm{T}}\mathbf{P}\mathbf{K}^{\mathrm{T}}) = Tr[\mathbf{C}_{\underset{\sim}{z}}(\mathbf{K})\mathbf{P}\mathbf{C}_{\underset{\sim}{z}}^{\mathrm{T}}(\mathbf{K})] \tag{A.5}$$

where

$$\mathbf{C}_{\underset{\sim}{z}}(\mathbf{K}) = \begin{bmatrix} \mathbf{Q}^{1/2} - \Upsilon\mathbf{K} \\ \Upsilon^{\mathrm{T}} - \mathbf{R}^{1/2}\mathbf{K} \end{bmatrix} \tag{A.6}$$

for real symmetric matrices $\mathbf{Q}^{1/2}$ and $\mathbf{R}^{1/2}$. Note that there is not necessarily a unique Υ for a given $\mathbf{N}$ in (A.5). The gain in problem (19) can be found as

$$\mathbf{K}_0 = \arg \min_{\mathbf{K}} \; Tr[\mathbf{C}_{\underset{\sim}{z}}(\mathbf{K})\mathbf{P}_0(\mathbf{K})\mathbf{C}_{\underset{\sim}{z}}(\mathbf{K})] \tag{A.7}$$

where

$$\mathbf{P}_0(\mathbf{K}) = [\mathbf{P} \mid \mathbf{A}_{\mathrm{c}}(\mathbf{K})\mathbf{P} + \mathbf{P}\mathbf{A}_{\mathrm{c}}^{\mathrm{T}}(\mathbf{K}) + \mathbf{E}\mathbf{E}^{\mathrm{T}} = 0] \quad \text{and} \quad \mathbf{A}_{\mathrm{c}}(\mathbf{K}) = \mathbf{A} - \mathbf{B}\mathbf{K}. \tag{A.8}$$

Similarly, the gain in problem (20) can be written as

$$\mathbf{F}_0 = \arg \min_{\mathbf{F}} \; Tr[\mathbf{C}_{\underset{\sim}{z}}(\mathbf{F})\mathbf{S}_0(\mathbf{F})\mathbf{C}_{\underset{\sim}{z}}(\mathbf{F})] \tag{A.9}$$

where

$$\mathbf{S}_0(\mathbf{F}) = \arg \min_{\mathbf{S}} Tr[\mathbf{C}_{\underline{z}}(\mathbf{F})\mathbf{S}\mathbf{C}_{\underline{z}}^{\mathrm{T}}(\mathbf{F})] \quad \text{subject to } \mathbf{A}_{\mathrm{c}}(\mathbf{F})\mathbf{S} + \mathbf{S}\mathbf{A}_{\mathrm{c}}^{\mathrm{T}}(\mathbf{F}) + \mathbf{E}\mathbf{E}^{\mathrm{T}} \le 0 \quad \text{and} \quad \mathbf{A}_{\mathrm{c}}(\mathbf{F}) = \mathbf{A} - \mathbf{B}\mathbf{F}. \tag{A.10}$$

Using Lemma A.7, one can show that the matrix functions given by equations (A.8) and (A.10) are equal. Therefore, $\mathbf{K}_0 = \mathbf{F}_0$ and $\mathbf{P}_0(\mathbf{K}_0) = \mathbf{S}_0(\mathbf{F}_0)$. Note that a strict inequality is used in (20) while (A.10) is a semidefinite problem. As discussed before, from a numerical point of view, the strict and nonstrict versions of the inequalities do not make a difference in the solutions.

The main difference between the problems (19) and (20) — *i.e.*, the inequality condition — allows one to add additional constraints to the LQR problem. It is clear that the addition of a new constraint will result in $\mathbf{S}_0 \ge \mathbf{P}_0$. Therefore, the solution of (20) with additional inequality constraints is expected to give larger outputs (though possibly a more robust controller) than a standard LQR. This concept can also be used to explain the difference between active and semiactive control. Let $\mathbf{S}_{\mathrm{d}}$ and $\mathbf{P}_0$ be the Lyapunov matrices obtained from the LQR problem with the dissipativity constraint and without it. For $\mathbf{S}_{\mathrm{d}}$ to be equal to $\mathbf{P}_0$, the Lyapunov dissipativity must be equal to the mean closed-loop dissipativity, which is practically impossible if higher mean dissipativity is desired. A high dissipativity will result in $\mathbf{S}_{\mathrm{d}} > \mathbf{P}_0$, *i.e.*, increased outputs and robustness.

APPENDIX III. REFERENCES

Boyd, S., Ghaoui, L. E., Feron, E., and Balakrishnan, V. (1994). *Linear Matrix Inequalities in System and Control Theory*, Studies in Applied Mathematics, **15**, SIAM, Philadelphia, Pennsylvania.

Chen, C.-T. (1999). *Linear System Theory and Design*, Oxford University, New York.

Christenson, R. E. (2003). "Probabilistic approach to assess the applicability of smart damping technology." *CD-ROM Proceedings of 16th ASCE Engineering Mechanics Conference*, Seattle, Washington.

Dullerud, G. E., and Paganini, F. (2000). *A Course in Robust Control Theory: A Convex Approach*, Springer, New York.

Dyke, S. J., Spencer, B. F., Jr., Sain, M. K., and Carlson J. D. (1996). "Modeling and control of magnetorheological dampers for seismic response reduction." *Smart Materials & Structures*, **5**(5), 565–575.

Dyke, S. J., Spencer, B. F., Jr., Sain, M. K., and Carlson J. D. (1998). "An experimental study of MR dampers for seismic protection." *Smart Materials and Structures*, **7**(5), 693–703.

Erkus, B., Abé, M, and Fujino, Y. (2002). "Investigation of semi-active control for seismic protection of elevated highway bridges." *Engineering Structures*, **24**(3), 281–293.

Feron, E., Balakrishnan, V., Boyd, S., and El Ghaoui, L. (1992). "Numerical methods for H_2 related problems." *Proceedings of American Control Conference*, Chicago, Illinois, 2921–2922.

Gahinet, P., Nemirovski, A., Laub., A. J., and Chilali, M. (1995). *LMI Control Toolbox*. MathWorks, Natick, Massachusetts.

Gurtin M. E., and Herrera I. (1964). "On dissipation inequalities and linear viscoelasticity." *Division of Applied Mathematics Technical Report Nonr-562(25)/27*, Brown University, Providence, Rhode Island.

Inaudi, J. A. (2000). "Performance of variable-damping systems: Theoretical Analysis and Simulation." *Proceedings of 3rd International Workshop on Structural Control*, Paris, France, 301–316.

Ioannou, P. A., and Tao, G. (1987). "Frequency domain conditions for strictly positive functions." *IEEE Transactions on Automatic Control*, 32(**1**), 53–54.

Johnson, E. A., Baker, G. A., Spencer, B. F., Jr., and Fujino, Y. (2004). "Semiactive damping of stay cables." *Journal of Engineering Mechanics*, ASCE, *in press.*

Johnson, E. A. (2000). "Nonlinear seismic benchmark problem: Dissipativity and the 9-Story benchmark building." *Proceedings of 2nd European Conference on Structural Control*, Champs-sur-Marne, France.

Housner, G. W., Bergman, L. A., Caughey, T. K., Chassiakos, A. G., Claus, R. O., Masri, S. F., Skelton, R. E., Soong, T. T., Spencer, B. F., Jr., and Yao, T. P. (1997). "Structural control: past, present, and future." *Journal of Engineering Mechanics*, ASCE, **123**(9), 897–971.

Khargonekar, P. P., and Rotea, M. A. (1991). "Mixed H_2/H_∞ control: A convex optimization approach." *IEEE Transactions on Automatic Control*, **36**(7), 824–837.

Masubuchi, I., Ohara, A., and Suda, N. (1998). "LMI-based controller synthesis: A unified formulation and solution." *International Journal of Robust Nonlinear Control*, **8**(8), 669–686.

Nesterov, Y., and Nemirovskii, A. (1994). *Interior-point Polynomial Algorithms in Convex Programming*, Studies in Applied Mathematics, **13**, SIAM, Philadelphia, Pennsylvania.

Peres P. L. D., Souza, S. R., and Geromel, J. C. (1992). "Optimal H_2 control for uncertain linear systems." *Proceedings of American Control Conference*, Chicago, Illinois, 2916–2920.

Ramallo, J. C., Johnson, E. A., and Spencer, B. F., Jr. (2002). "'Smart' base isolation systems." *Journal of Engineering Mechanics*, ASCE, **128**(10), 1088–1099.

Safonov, M. G., Goh, K. C., and Ly, J. H. (1994). "Control system synthesis via bilinear matrix inequalities." *Proceedings of American Control Conference*, Baltimore, Maryland, 45–49.

Scherer, C., Gahinet, P., and Chilali, M. (1997). "Multiobjective output-feedback control via LMI optimization." *IEEE Transactions on Automatic Control*, **42**(7), 896–911.

Slotine, J.-J. E., and Li, W. (1991). *Applied Nonlinear Control*. Prentice-Hall, Englewood Cliffs, New-Jersey.

Soong, T. T., and Spencer, B. F., Jr. (2002). "Supplemental energy dissipation: State-of-the-art and state-of-the-practice." *Engineering Structures*, **24**(3), 243–259.

Spencer, B. F., Jr., and Sain, M. K. (1997). "Controlling buildings: A new frontier in feedback." *IEEE Control Systems Magazine*, **17(**6), 19–35.

Spencer, B. F., Jr., Johnson, E. A., and Ramallo, J. C. (2000). "'Smart' isolation for seismic control." *JSME International Journal*, Series C, **43**(3), 704–711.

Symans, M. D., and Constantinou, M. C. (1999). "Semi-active control systems for seismic protection of structures: A state-of-the-art review." *Engineering Structures*, **21**(6), 469–487.

Taylor, J. H. (1974). "Strictly positive-real functions and the Lefschetz-Kalman-Yakubovich Lemma." *IEEE Transactions on Circuits and Systems*, **21**(2), 310–311.

Toker, O., and Özbay, H. (1995). "On the $\mathcal{NP}$-hardness of solving bilinear matrix inequalities and simultaneous stabilization with static output feedback." *Proceedings of American Control Conference*, Seattle, Washington, 2525–2526.

Turan, L., Safonov, M. G., and Huang, C. H. (1997). "Synthesis of positive real feedback systems: A simple derivation via Parrott's theorem." *IEEE Transactions on Automatic Control*, **42**(8), 1154–1157.

Wen, J. T. (1988). "Time domain and frequency domain conditions for strict positive realness." *IEEE Transactions on Automatic Control*, **33**(10), 988–992.

Willems, J. C. (1971). "Least squares stationary optimal control and the algebraic Ricatti equation." *IEEE Transactions on Automatic Control*, **AC-16**(6), 621–634.

Willems, J. C. (1972a). "Dissipative dynamical systems – Part I: General theory." *Archive for Rational Mechanics and Analysis*, **45**(5), 321–351.

Willems, J. C. (1972b). "Dissipative dynamical systems – Part II: Linear systems with quadratic supply rates." *Archive for Rational Mechanics and Analysis*, **45**(5), 352–393.

Yang, G., Spencer, B. F., Jr., Carlson J. D. and Sain, M. K. (2002). "Large-scale MR fluid dampers: modeling and dynamic performance considerations." *Engineering Structures*, **24**(3), 309–323.

Yang, J. N., Lin, S. and Jabbari, F. (2003). "H_2-based control strategies for civil engineering structures." *Journal of Structural Control*, **10**(3–4), 205–230.

Yang, J. N., Lin, S. and Jabbari, F. (2004). "Linear Multiobjective Control Strategies for Wind-Excited Buildings." *Journal of Engineering Mechanics*, ASCE, **130**(4), 471–477.